

Thermoelectric Magnetohydrodynamic and Thermocapillary Driven Flows in Liquid Conductors in Magnetic Fields

Michael Andrew Jaworski

Department of Nuclear, Plasma and Radiological Engineering
University of Illinois at Urbana-Champaign

Correspondence: mjaworsk@illinois.edu

Acknowledgments

- Hard working undergraduates: Mike Antonelli, Chuck Lau, Matt Lee, Jason Kim, Jerry Klosek, and David Urbansky
- Fellow graduate students: Wenyu Xu, Travis Gray, Eithan Ritz
- Thesis committee: David Ruzic (chair, NPRE), Barclay Jones (NPRE), George Miley (NPRE), Angus Rockett (MatSE) and Brian Thomas (MechSE)
- CPMI staff: Dr. Martin Neumann
- Colleagues in the field: R. Kaita, R. Majeski and N.B. Morley
- Funding: Department of Energy contract:
 - DE-FG02-99ER54515

Overview

A theory explaining the balance between thermoelectric magnetohydrodynamics (TEMHD) and thermocapillary (TC) driven, free-surface flows in containers of arbitrary type in a magnetized environment has been developed. A new dimensionless group depending on the thermoelectric power of the liquid/container pair, the physical properties of the liquid and solid and the flow geometry has been found that determines which mechanism, TC or TEMHD, is the dominant effect in any given system.

The Solid/Liquid Lithium Divertor Experiment (SLiDE) has been constructed and operated to experimentally test thermally driven flows in liquid lithium. Results are in qualitative agreement with the developed theory and constitute the first direct observation of TEMHD driven flow yet reported. Technologies suggested by TEMHD are also discussed.

Outline

- Introduction – Motivation, concept history and present knowledge on the topic
 - Genesis
 - Motivation and history
 - Thermocapillary and thermoelectric MHD driven flows
 - Goals of the present work
- Theory – Thermocapillary and TEMHD driven flows in “open geometries” and the SLiDE machine
- Apparatus – Machine overview and operation
- Results – Qualitative experiments and quantitative measurements
- Discussion – Understanding drawn from experimental results
- Conclusions - Summary



Genesis

- CDX-U machine in 2005 presented remarkable results
 - Liquid lithium could handle an intense electron beam heat flux (50 MW/m²) without evaporating
 - Melted entire tray with local spot heating
 - Observed surface flow during operation
- Questions instantly raised:
 - What is the mechanism behind the flow?
 - How does the effect scale with magnetic field?
 - Can this be used as a fusion divertor?



Courtesy R. Majeski and R. Kaita, PPPL

First question in this talk:

Why are they using liquid lithium and why is this an interesting result?



Motivation: No Solution in Hand

- Panel report to Fusion Energy Sciences Advisory Committee was commissioned to identify “gaps” in present knowledge between present knowledge and a Demonstration reactor
- They classified the plasma facing components (PFCs) and materials in a fusion reactor as having “Tier 1” priority:
 - **“Tier 1: solution not in hand, major extrapolation from current state of knowledge, need for qualitative improvements and substantial development for both short and long term.”** (p. 12 “Greenwald” Report)
- In identifying potential solutions and research paths, the panel had this to say as well:
 - **Liquid surface PFCs are a “high-risk high-reward alternative to solid PFCs in Demo.”** (p. 175, *ibid.*)
- In particular, liquid lithium has been identified as having several advantages

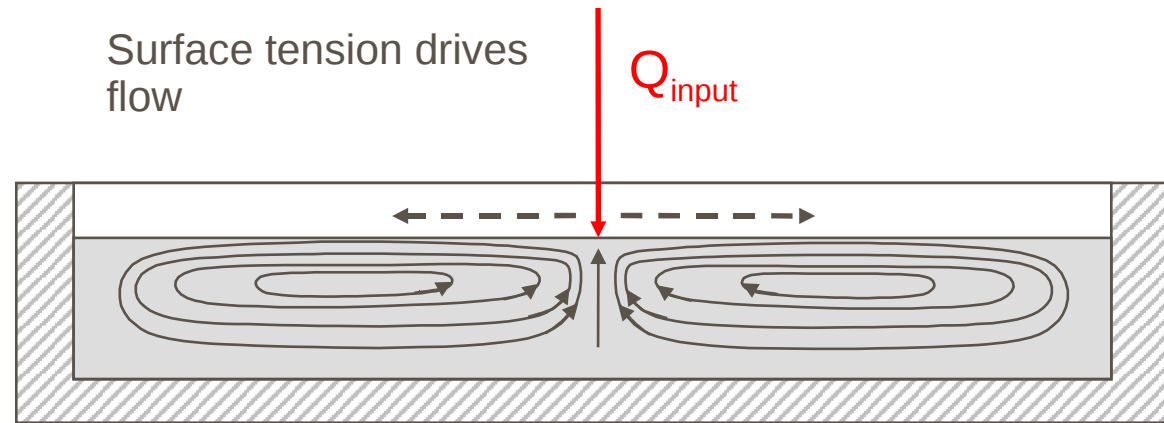
Liquid Surface PFCs

- Continuously replenishing surface
 - No long term erosion problems
 - No permanent damage to the PFC
 - No thermo-mechanical stress or fatigue in the PFC itself
- Liquid lithium specific advantages
 - Tritium inventory control – getters hydrogen and isotopes, control the lithium and control the fuel
 - Improved plasma performance
 - Low Z material pollutes less when inside the plasma
 - Getters other impurities as well
- Liquid lithium disadvantage: evaporates rapidly at relatively low temperatures (350-400 C considered limit in fusion machines)



Thermocapillary Flow, Basics

- Proposed solution to the CDX-U mystery
- Thermocapillary
 - “Thermo” meaning temperature
 - “Capillary” meaning related to surface tension
 - Temperature gradient on surface of a liquid creates surface tension gradients
 - Surface tension gradients result in flow generation
- Long history of study from mid-19th century



- Surface tension origins
 - Intermolecular forces attract molecules to one another
 - Free-surface results in net inward force – no molecules to be attracted to above surface
 - Results in surface energy or force per length that pulls surface into minimum energy shape



Thermoelectric MHD, Basics

- Thermoelectric effect
 - Causes thermocouple junction voltages
 - Thermoelectric power present in most materials
 - Electromotive force generated by temperature gradients
 - Requires different material (or TE power) to provide current return path and generate current
 - Arises from lack of thermodynamic equilibrium in a material's conduction electrons in temperature gradients
- Replace one material with a liquid in magnetic field
 - TE current and B-field generate Lorentz force
- First formal exposition of TEMHD in 1979
 - Shercliff, 1979 proposed the use of TEMHD as pumping mechanism
 - Highlighted liquid lithium in fusion context
- Scant development since 1979
 - Crystal growth experiments found indirect evidence
 - Metallurgical studies looking at grain structure found indirect evidence of TEMHD flows
 - NO work in fusion since introduction in 1979



Purpose of this Work

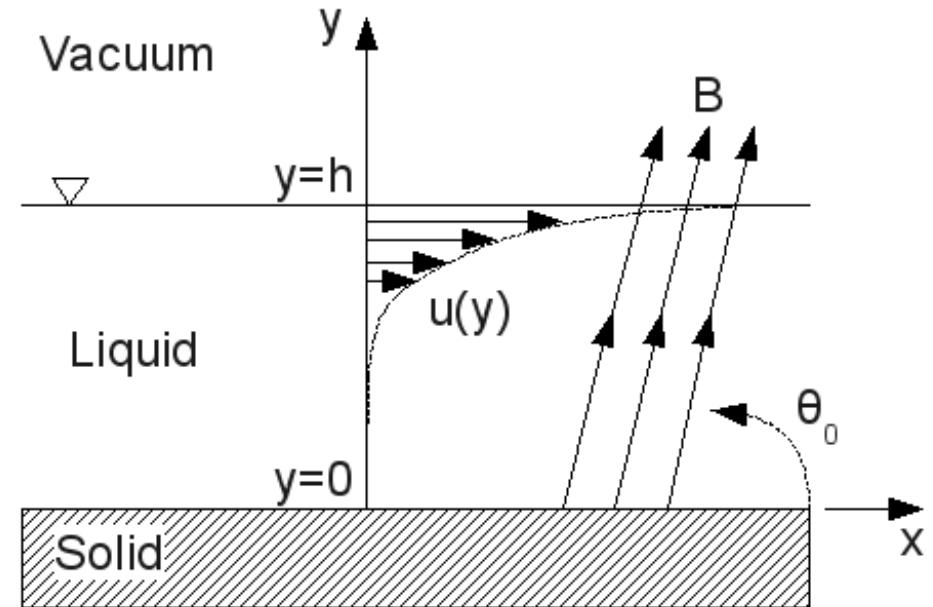
- Understand the mechanism behind the motion of the liquid lithium observed in CDX-U
- Identify relevant parameters controlling this effect
- Determine the magnitude of this effect and its scaling
- Verify with an experiment

Theory: Outline

- Thermocapillary MHD flows
 - Formulation
 - Solution with and without return flow
- TEMHD flows
 - Equations of motion and boundary conditions
 - Solution in an “open” geometry
 - Swirling flow solution
- Thermal hydraulic implications of flow

Thermocapillary MHD

- Consider a semi-infinite domain
 - Free-surface at $y=h$
 - Magnetic field B
 - Surface subject to constant temperature gradient b
- Two cases
 - No return flow ($dP/dx = 0$)
 - Return flow (dP/dx related to height of the fluid)
- Surface tension boundary condition
 - Surface tension gradient results in viscous shear at surface



$$\nabla \cdot \mathbf{V} = 0$$

$$\rho \frac{D\mathbf{V}}{Dt} = -\nabla P + \mu \nabla^2 \mathbf{V} + \rho \mathbf{g} + \mathbf{J} \times \mathbf{B}$$

$$\rho C_p \frac{DT}{Dt} = k \nabla^2 T + \Pi + \frac{\mathbf{J} \cdot \mathbf{J}}{\sigma}$$

$$\Sigma(T) = \Sigma_0 - \gamma(T - T_0)$$

$$\mu \left. \frac{du}{dy} \right|_{y=h_0} = \left. \frac{\partial \Sigma}{\partial x} \right|_{y=h_0}$$

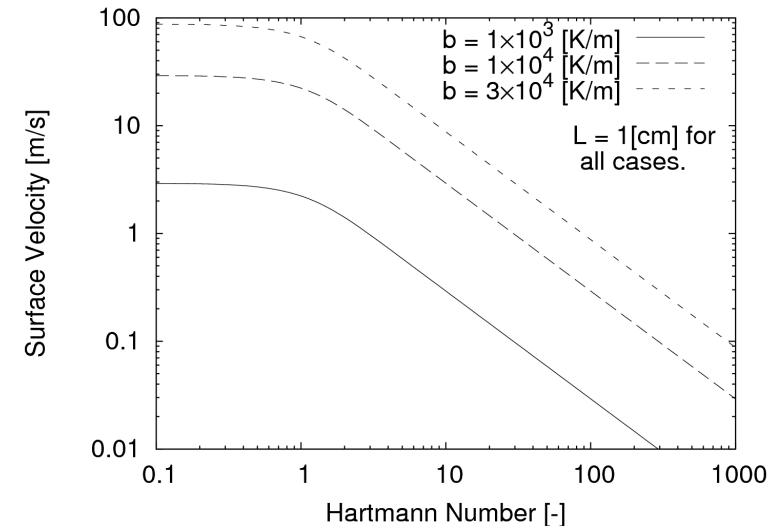
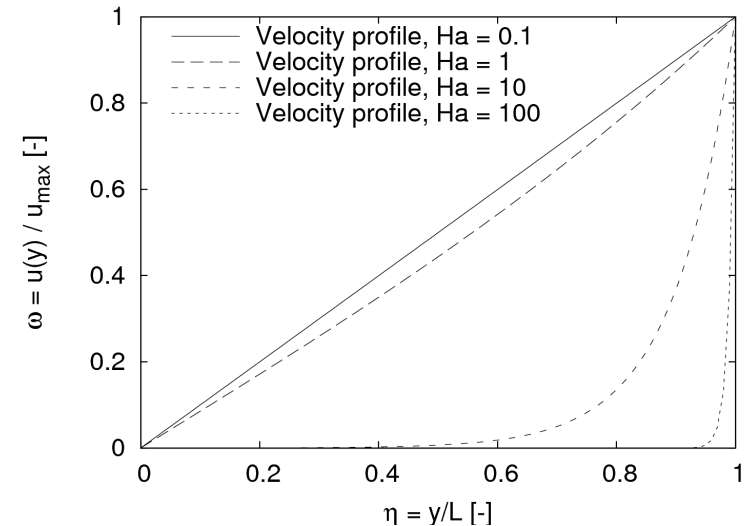
Solution 1: No Return Flow

- Solution depends on similarity variables
 - Hartmann No. is ratio btw magnetic and viscous damping
 - Marangoni No. is ratio of surface tension to viscous forces
- Velocity limited to Hartmann layer near surface
 - Significant velocities developed
 - Damp quickly with magnetic field (turn over at $Ha = 1$)

$$u_{max} = \frac{\alpha}{h_0} \cdot \frac{\mathfrak{M}}{\xi} \tanh \xi$$

$$\xi = h_0 B_y \left(\frac{\sigma}{\rho \nu} \right)^{1/2} \quad \text{Hartmann}$$

$$\mathfrak{M} = \frac{\gamma b h_0^2}{\rho \nu \alpha} \quad \text{Marangoni}$$

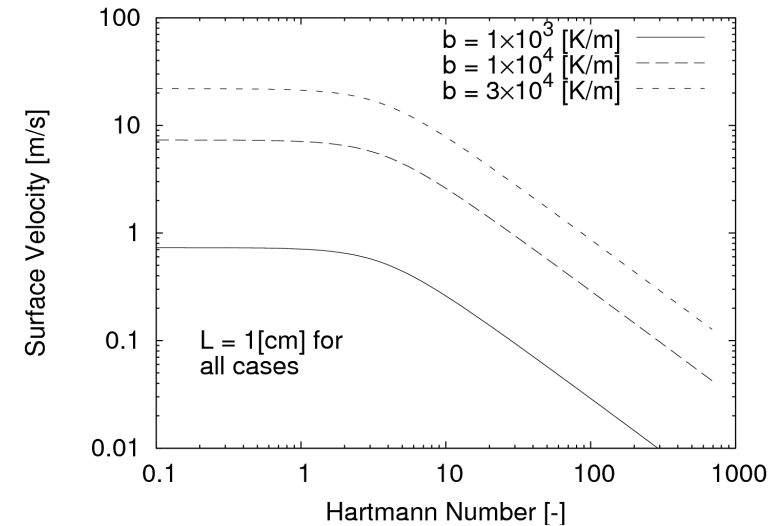
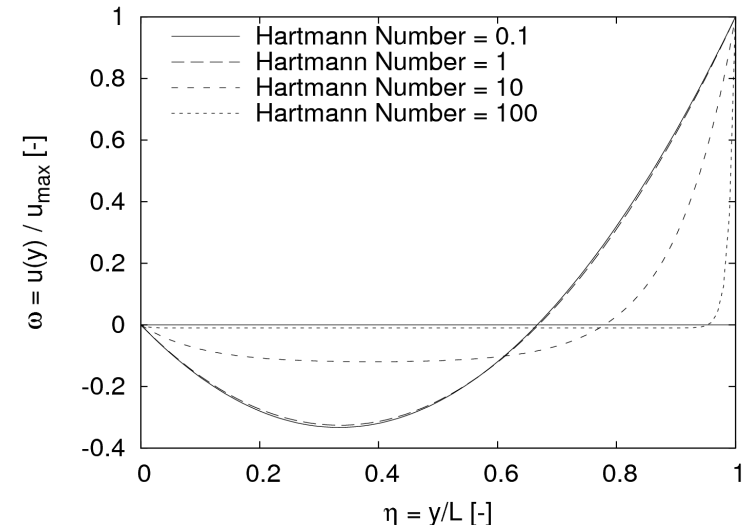


Solution 2: Return Flow

- Return flow solution
 - Change in height produces return pressure
 - Flow turn-around assumed “far” from area of interest
- Solution still dependent on two similarity variables
 - Highest velocities still limited to Hartmann layer at surface
 - Slow return flow in the bulk due to pressure
 - High Hartmann limit reduces to no-return solution

$$P(x, y) = P_0 + \rho g [h(x) - y]$$

$$u_{max} = \frac{\alpha}{h_0} \cdot \frac{\mathfrak{M}}{\xi} \left(\frac{2 - 2 \cosh(\xi) + \xi \sinh(\xi)}{\xi \cosh(\xi) - \sinh(\xi)} \right)$$

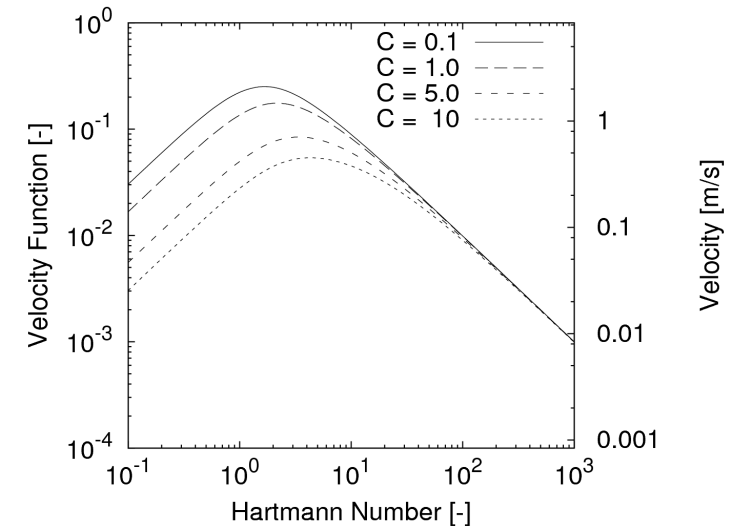
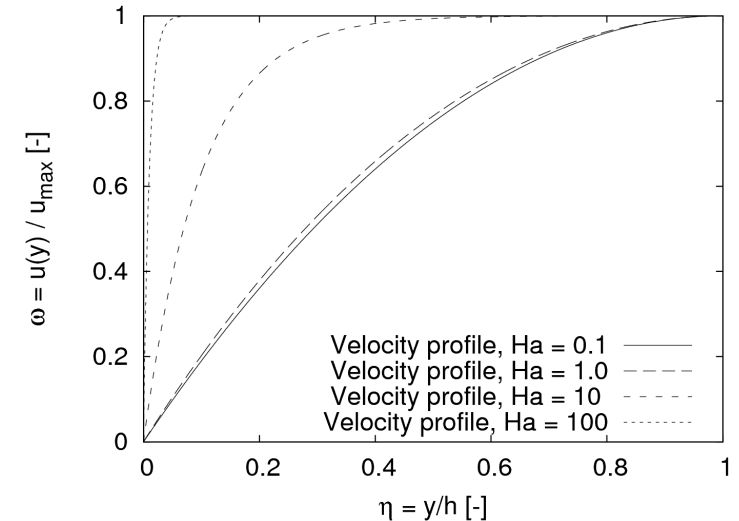


TEMHD Solution 1: Semi-Infinite Domain

- Similar geometry to TC flow
- Solution for free surface
 - Identical to Shercliff, 1979 channel flow
 - Lithium-Iron example: $P = 20e-6[V/K]$, $h=5[mm]$, $dT/dy = 1000[K/m]$
 - Pre-factor = $8.4[m/s]$
- Solution depends on several factors
 - Hartmann again present
 - “C” is ratio of liquid/wall impedances
 - “Pre-factor” and velocity function {...}

$$C = \frac{h\sigma}{t\sigma_w}$$

$$\begin{aligned} \bar{u} &= \frac{P}{B} \frac{dT}{dz} \left[\frac{\xi - \tanh(\xi)}{\xi + C \tanh(\xi)} \right] \\ &= Ph \left(\frac{\sigma}{\rho\nu} \right)^{1/2} \frac{dT}{dy} \left\{ \frac{\xi - \tanh(\xi)}{\xi[\xi + C \tanh(\xi)]} \right\} \end{aligned}$$

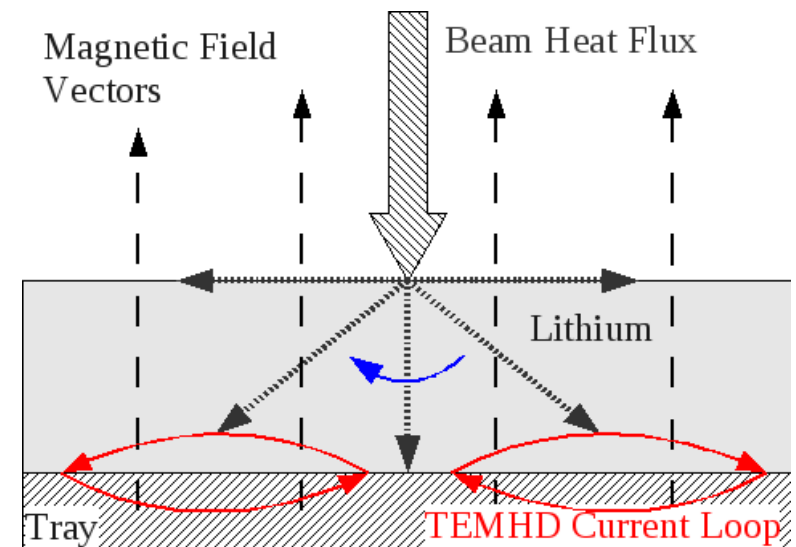
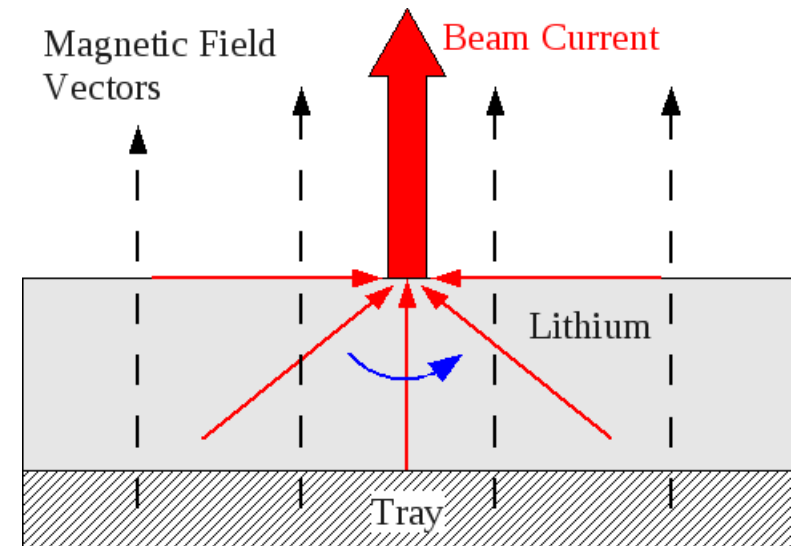


$$\mathbf{J} = \sigma (\mathbf{E} + \mathbf{u} \times \mathbf{B} - S\nabla T)$$



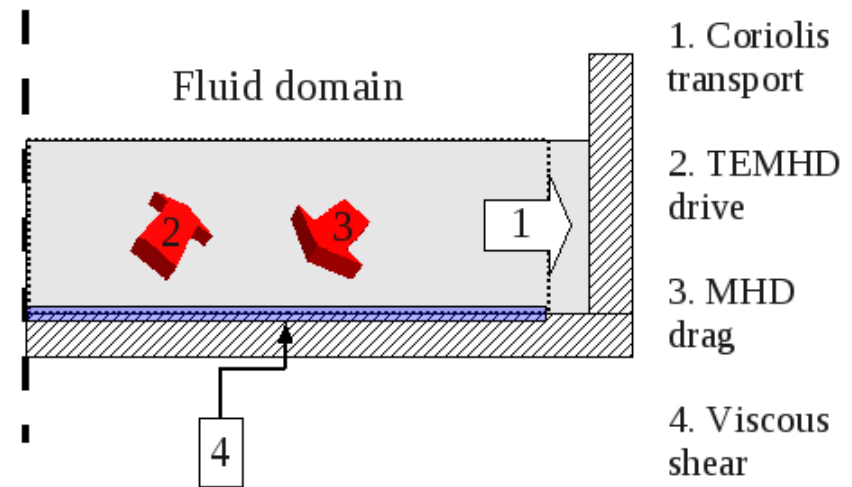
Swirling Flow by Beam and TE Currents

- **$\mathbf{J} \times \mathbf{B}$** forces result in swirling flow
 - Electron beam current concentrates inward
 - TE current flows outward (anti-parallel to temp. grad)
 - Result in opposite senses of rotation
- Swirling flow complicates original picture
 - Primary flow is around axis
 - Secondary flow is created which circulates in r - z plane



Torque Balance

- Apply conservation of angular momentum to control volume
 - Coriolis force arises from term on left – transport of angular momentum radially
 - MHD and TEMHD comprise body forces
 - Shear along the wall is last term on right
- Control volume simplifies
 - No complex turn-around
 - Coriolis is non-zero to account for transport out the right boundary
- Use approximate solutions for boundary layer flow (F and G)



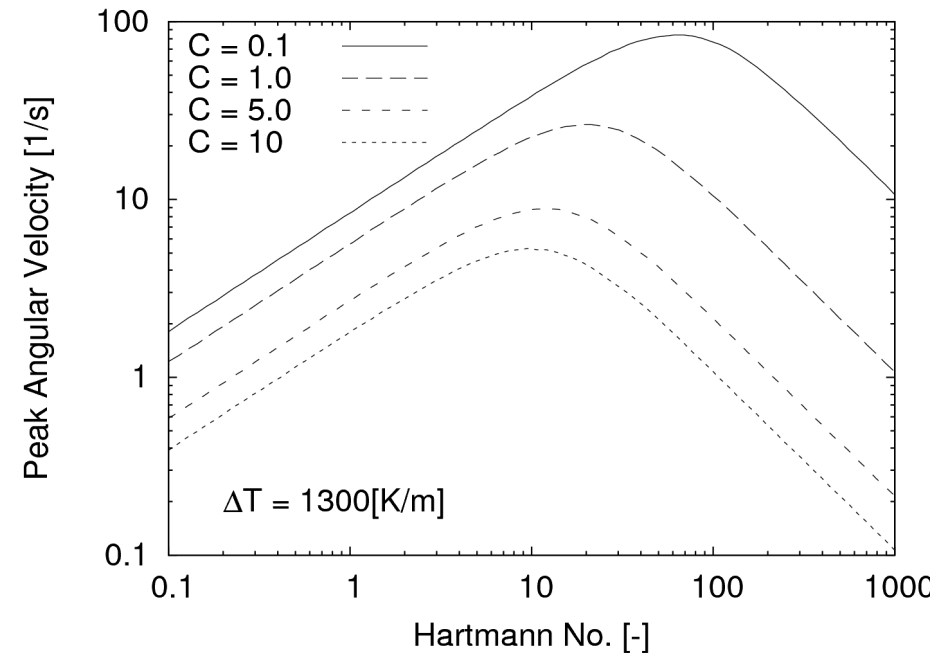
$$\oint_S (\rho \Gamma) \mathbf{u} \cdot d\mathbf{S} = \int_V (F_\phi r) dV + \oint_S r \tau_\phi \cdot d\mathbf{S}$$

$$\begin{aligned} e.g. \quad \oint_S (\rho \Gamma) \mathbf{u} \cdot d\mathbf{S} &= \int_0^{2\pi} \int_0^h \rho u_\phi(r) r u_r(r) dz \\ &= 2\pi \rho \int_0^h \Omega^2 r^3 F G dz \\ &= 2\pi \rho \Omega^2 r^3 \int_0^h F G dz \end{aligned}$$

$$\{\text{CORIOLIS}\} = \oint_S (\rho \Gamma) \mathbf{u} \cdot d\mathbf{S} = \frac{3}{2} \rho \nu^{1/2} \Omega^{3/2} \frac{R^4 \hat{R} + 2\hat{R}^2 \left(\hat{R} - H_\infty/2 \right)}{4 \left(1 + \hat{R}^2 \left(\hat{R} - H_\infty/2 \right)^2 \right)}$$

Result of Torque Balance

- Result of torque balance below
 - No closed form available
 - Solved numerically over range of magnetic fields
 - Solution depends on dimensionless impedance, C
 - Form of temperature gradient anticipates results



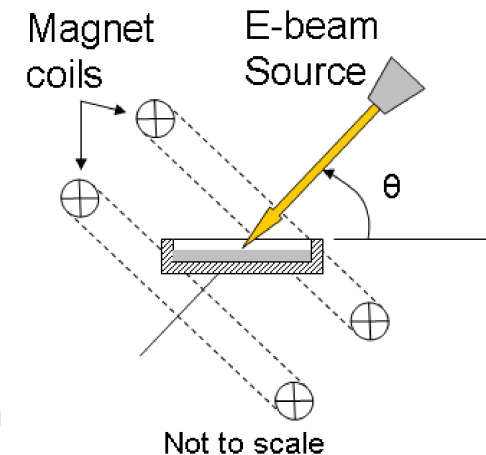
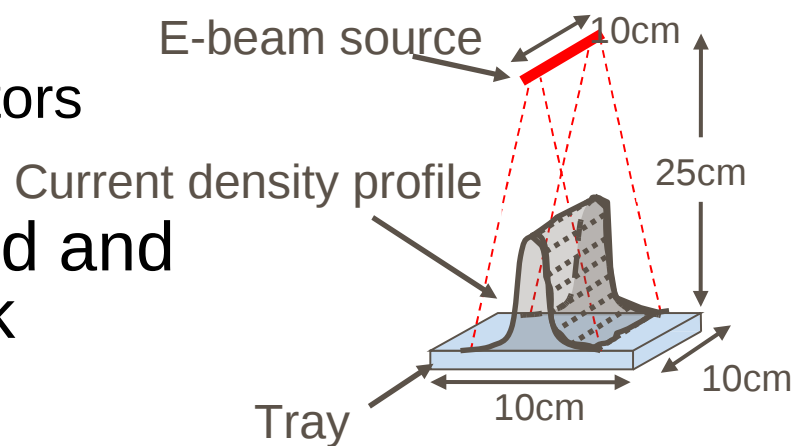
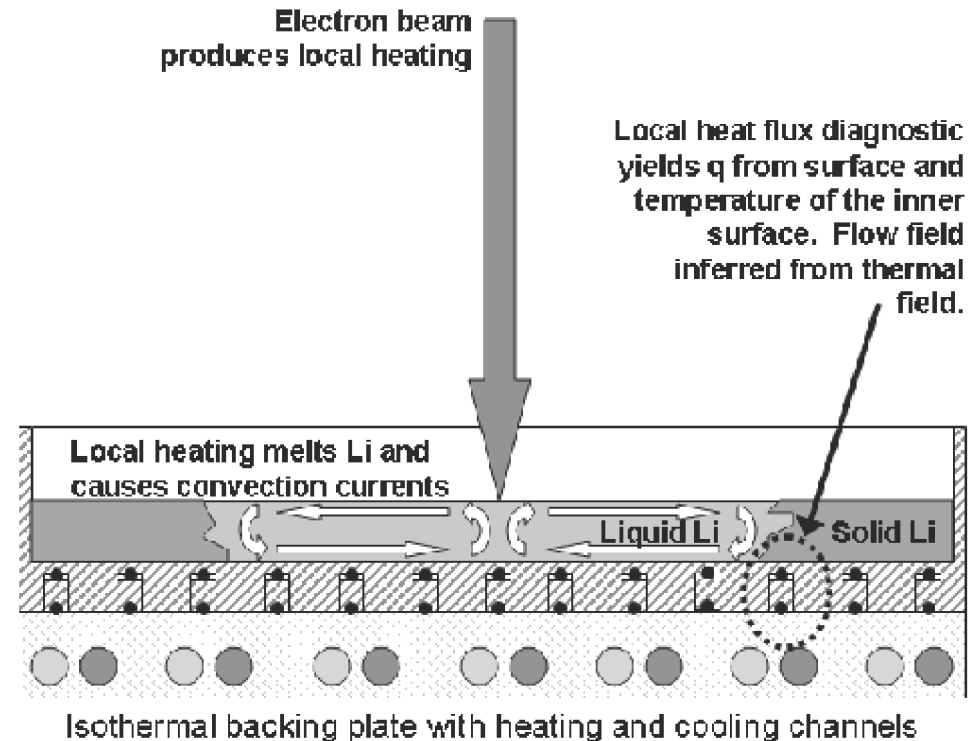
$$\begin{aligned}
 \{\text{TEMHD}\} &= \{\text{MHD}\} + \{\text{SHEAR}\} + \{\text{CORIOLIS}\} \\
 h \frac{\sigma B}{1+C} P(2A_2) &= \frac{C}{C+1} \sigma B^2 \left[\Omega h - (\Omega \nu)^{1/2} \frac{\hat{R}^2 (\hat{R} - H_\infty/2)}{1 + \hat{R}^2 (\hat{R} - H_\infty/2)^2} \right] + \dots \\
 &\dots \rho \nu \Omega \left(\hat{R} - \frac{H_\infty}{2} \right) + \dots \\
 &\dots \frac{3}{2} \rho \nu^{1/2} \Omega^{3/2} \frac{\hat{R} + 2\hat{R}^2 (\hat{R} - H_\infty/2)}{1 + \hat{R}^2 (\hat{R} - H_\infty/2)^2} \quad (2.111)
 \end{aligned}$$

Apparatus: Outline

- Machine overview – major components
- Electron beam – in brief
- Tray system – overview of system and performance
- Fourier model calibration with thermocouples
- Optics and camera system
- Data acquisition and control

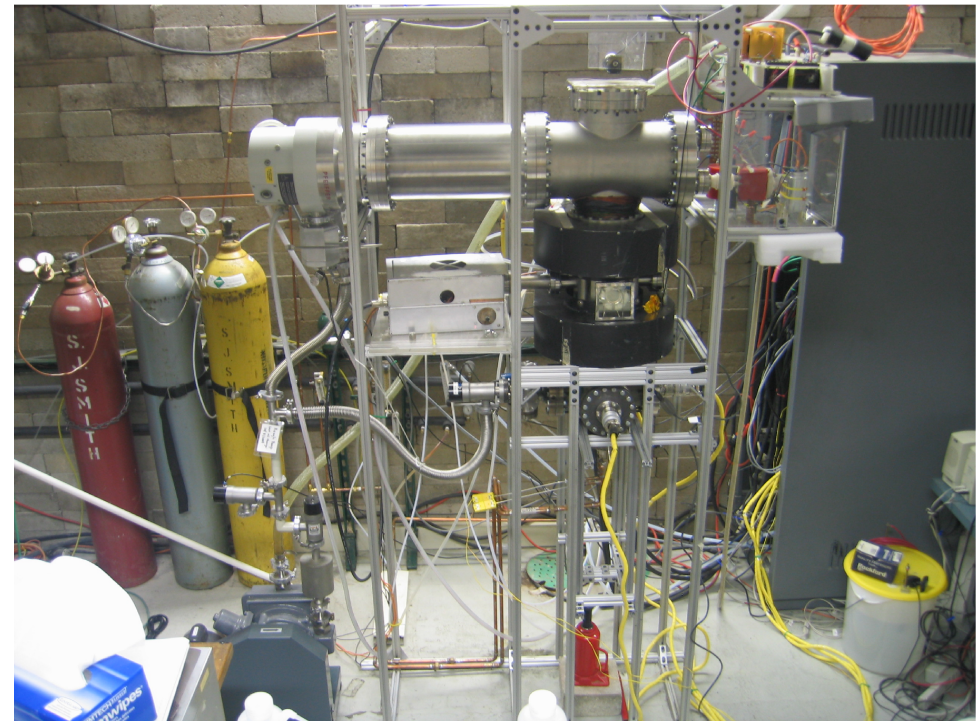
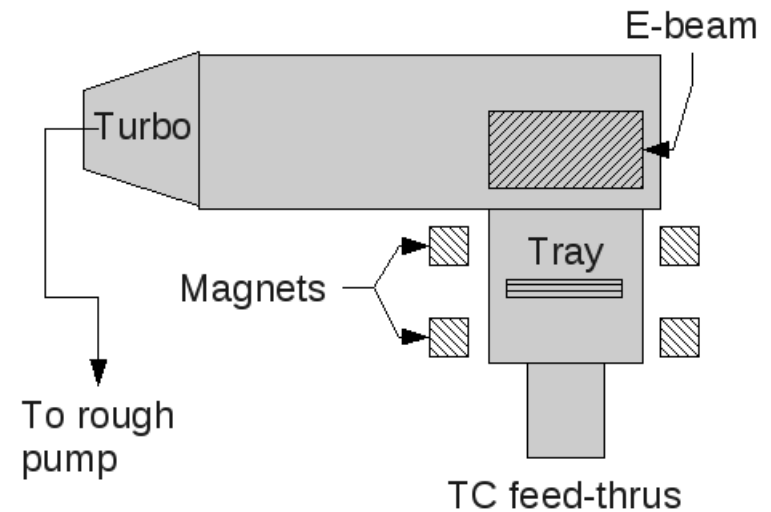
System Overview

- Solid/Liquid Lithium Divertor Experiment (SLiDE)
 - Produces temperature gradients with an electron beam
 - Creates magnetic field with external magnet system (these tests at normal incidence)
 - Measures temperature distribution in tray containing lithium
 - Active cooling for steady-state operation
 - Camera system monitors surface velocity
- Designed, constructed and operated for this work



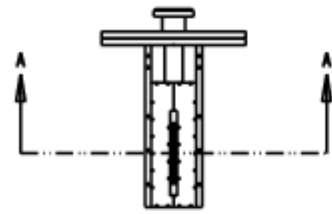
Machine Picture

- Main vacuum chamber and components shown here
 - System designed for maximum access
 - Black objects in near center of picture are magnets
- Control panel and computer not shown
 - Control rack at right of picture frame
 - Camera allows remote monitoring

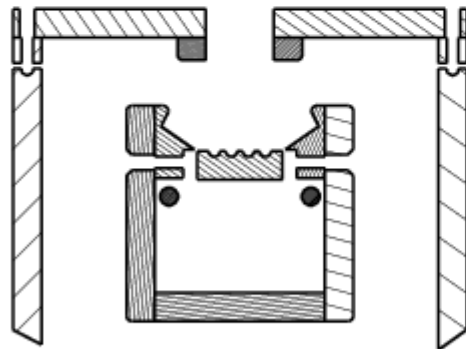
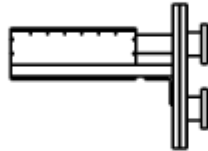


Electron Beam Drawings

PAGE 1 OF 26

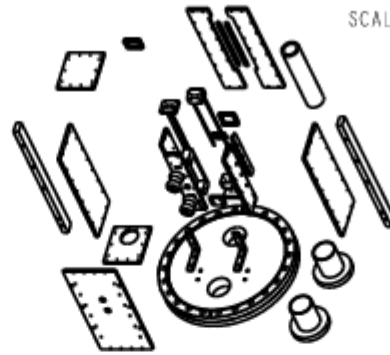


SEE DETAIL A

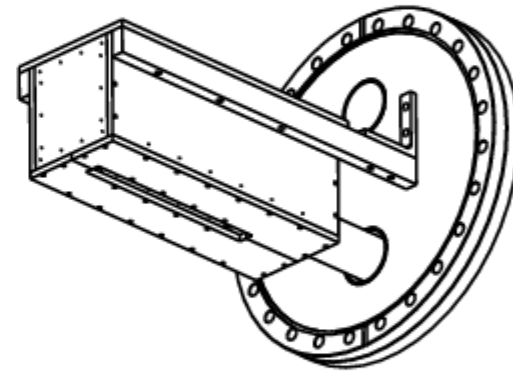


DETAIL A
SCALE 1.000

SECTION A-A
SCALE 0.100



SCALE 0.100



DESCRIPTION

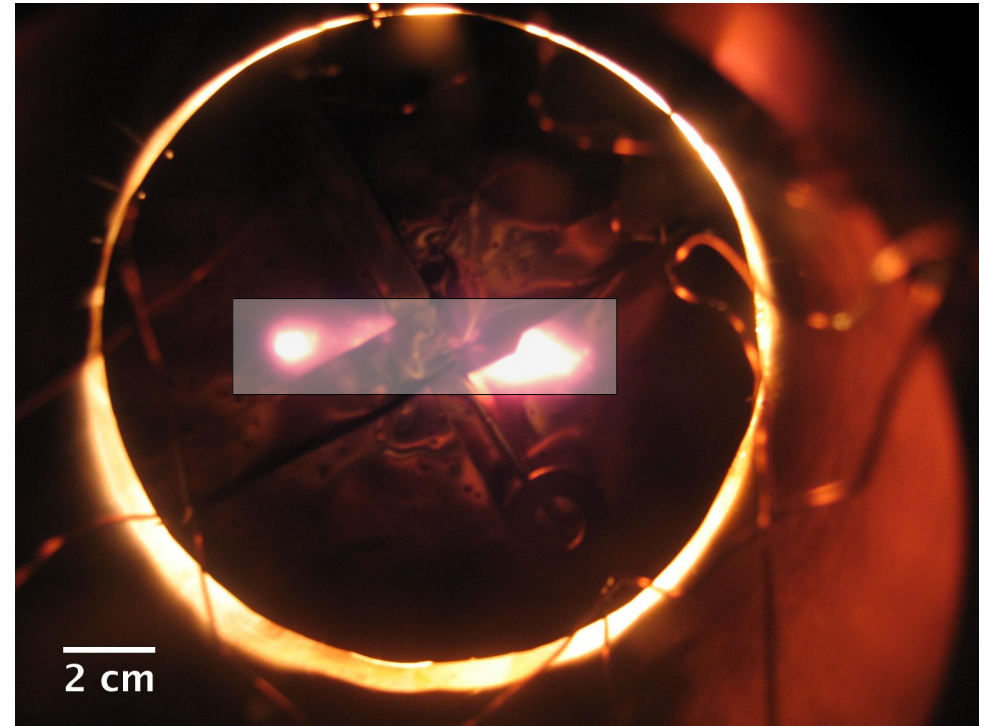
FULL ELECTRON BEAM ASSEMBLED OF BASE COMPONENTS.
ELECTRON BEAM MOUNTS TO FLANGE AND EXTENDS INTO CHAMBER.

CPMI SOLID/LIQUID LITHIUM DIVERTOR EXPERIMENT ELECTRON BEAM			
TITLE	E-BEAM ASSEMBLY	VERSION	1.1
NAME	M. A. JAWORSKI	DATE	07/25/08
UNITS	MILLIMETER (INCH)	MATERIAL	MULTIPLE
QTY	1	FILENAME	e-beam-assembly.drw



Electron Beam

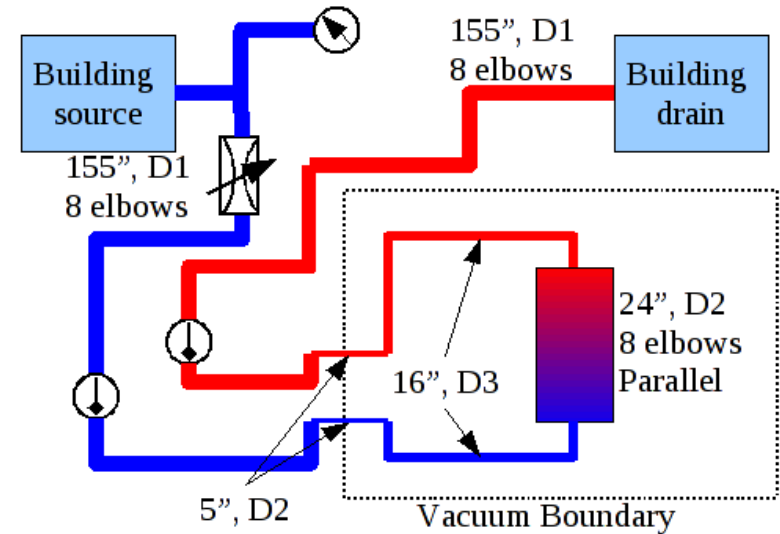
- Designed to mimic divertor heat flux
 - Actual run parameters shown in table
 - Operated at 300W in this set of experiments – capable of 15kW
 - Typical q_0 in NSTX is $\sim 10 \text{ MW/m}^2$
 - Typical dq/dx in NSTX is $\sim 100 \text{ MW/m}^2\text{-m}$
- Line source with gaussian profile
 - Mimics straightened divertor heat flux
 - Attempts to force 2D flow in TC cases



Magnetic Field B_0 [G]	Peak heat flux q_0 [MW/m ²]	Peak heat flux gradient (mean) $\partial q/\partial x$ [MW/m ² · m]
34	0.0668	1.96 (0.911)
68	0.096	3.66 (1.71)
135	0.116	4.8 (5.89)
271	0.196	12.6 (5.89)
406	0.225	17.7 (8.25)
542	0.648	143 (67.1)
677	0.683	162 (75.8)
778	0.709	176 (82.3)

Tray System Overview

- Coolant supplied from building sources
 - Water at 35 psi
 - Compressed air at 80 psi
 - Steady-state cooling with liquid lithium temperatures and input power range of 50W – 1500W (with stainless steel tray)
- 28 thermocouples within tray
 - 14 positions for heat flux modeling
 - 4 external TCs for coolant calorimetry



SCALE 0.300

BILL OF GOODS	
PART NAME	QTY
TRAY TOP ASSEMBLY	1
1/4"-28 UNF THREADED ROD	4
1/4"-28 UNF HEXNUT	24
BASE ATTACHMENT STAND	4
MSX.8 ISO 10MM BOLT	4
BASE ATTACHING FLANGE	1
SHORT PIPE ASSEMBLY	2
MID PIPE ASSEMBLY	1
LONG PIPE ASSEMBLY	1
ALIGNER WASHER	2

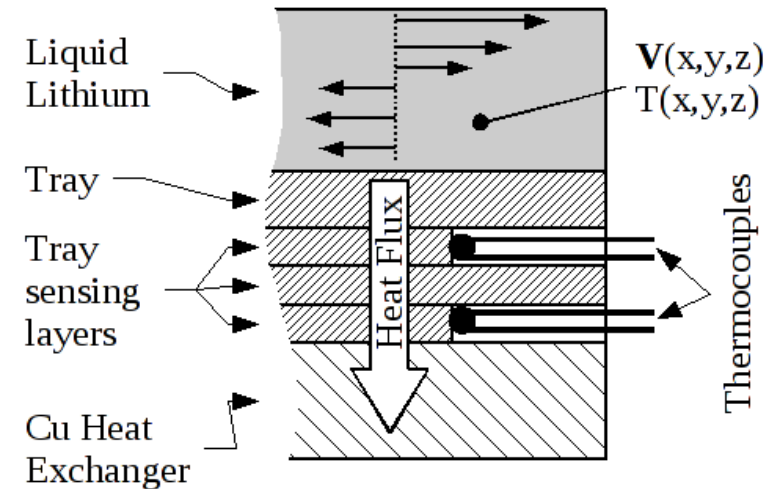
DESCRIPTION
 FULL TRAY ASSEMBLY FOR SLIDE APPARATUS. BASE ATTACHMENT STANDS MATE TO BASE ATTACHING FLANGE. THREADED RODS ATTACH TO STANDS AND ALIGNER PLATE OF THE TRAY TOP ASSEMBLY. SHORT, MID AND LONG PIPE ASSEMBLIES CREATED WITH STANDARD C. COMPRESSION FITTINGS AND COPPER TUBE.

SCALE 0.250

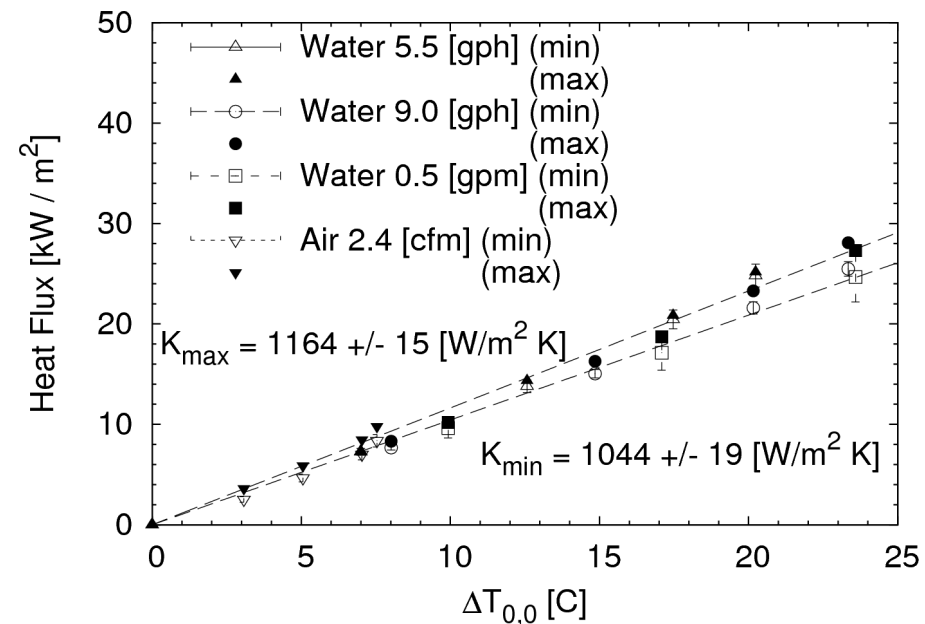
CPMI - SOLID/LIQUID DIVERTOR EXPERIMENT - TRAY			
TITLE	SLIDE TRAY ASSEMBLY	VERSION	1.2
NAME	M. A. JAWORSKI	DATE	10/23/2008
UNITS	MILLIMETERS (INCHES)	MATERIAL	MULTIPLE
QTY	1	FILENAME	FLANGE-TRAY-ASM.DRW

Heat Flux Model Calibration

- Fourier model of heat conduction used
 - Local heat flux determined by thermocouple pair
 - Calibration accounts for contact resistance
- Same model used to reconstruct interface temperature
 - Aluminum block temperature measurement used
 - Calibration of heat flux and effective distance to plate created for each of the 14 thermocouple pairs

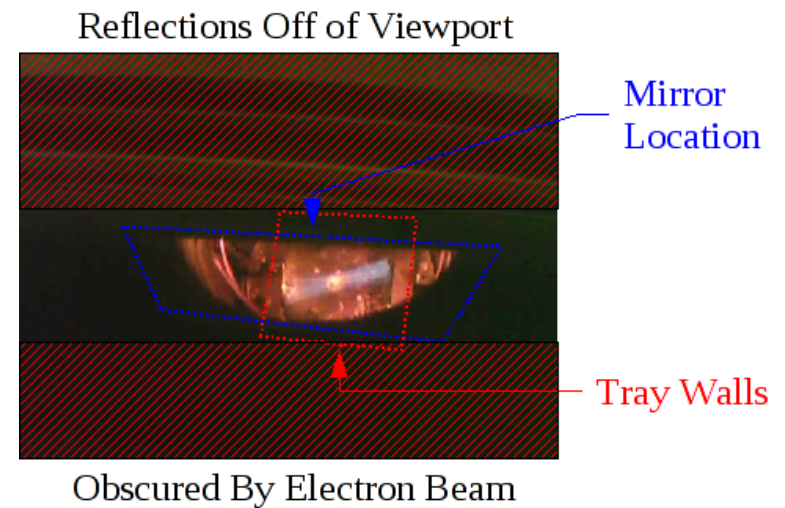
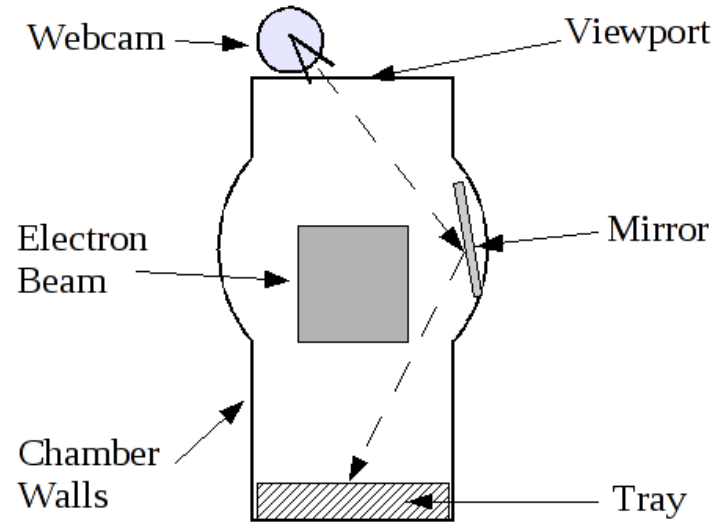


$$q_i = K_i(T_{i,top} - T_{i,bottom})$$



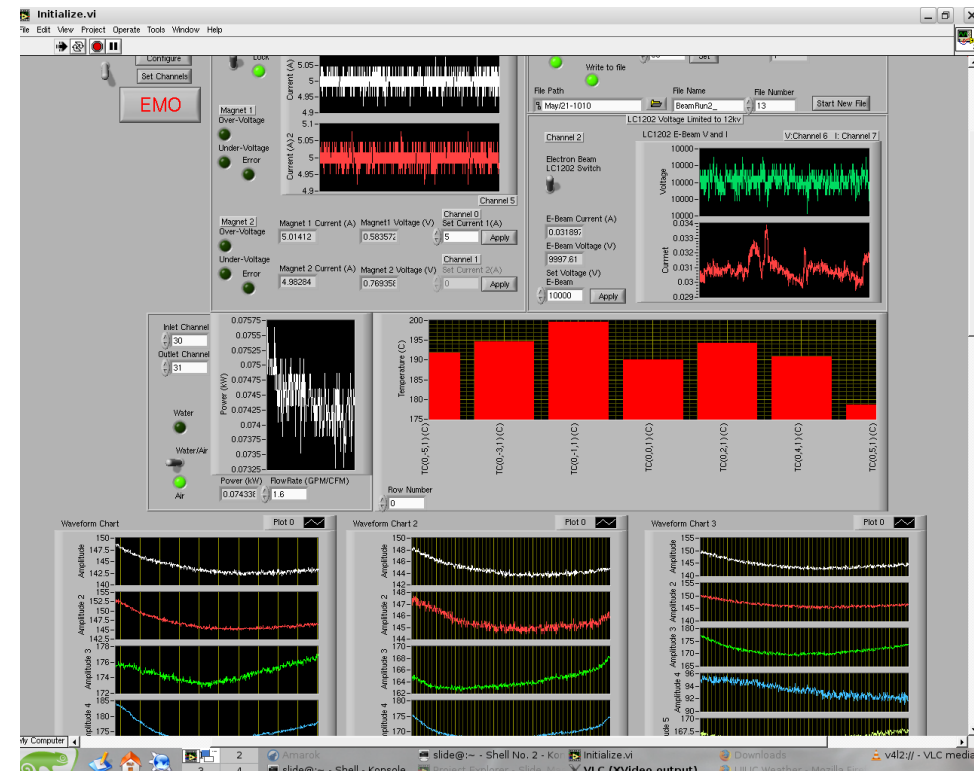
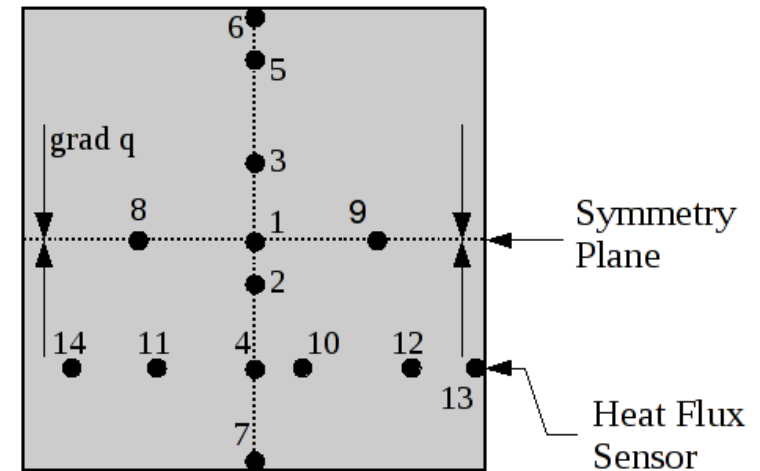
Camera System

- Mirror used to view lithium surface
 - Electron beam occludes direct view
 - Mirror requires periodic cleaning from lithium evaporation
- Two cameras used
 - Low quality webcam for simple monitoring
 - High quality, high-definition camera used for velocity measurement movies
 - Both utilize mirror
 - Illumination provided by electron beam filaments



Data Acquisition and Control

- Thermocouple data acquired via computer system
 - LABJACK USB data modules and amplifiers digitize analog signals
 - Homebrew LabVIEW VI monitors temperatures in real time
 - Control of magnets and eBeam voltage via computer system (filaments on manual)
- Post-run analysis handled semi-autonomously
 - Analysis program written to reference and analyze data sets
 - Output summarizes and formats for easy plotting and further analysis

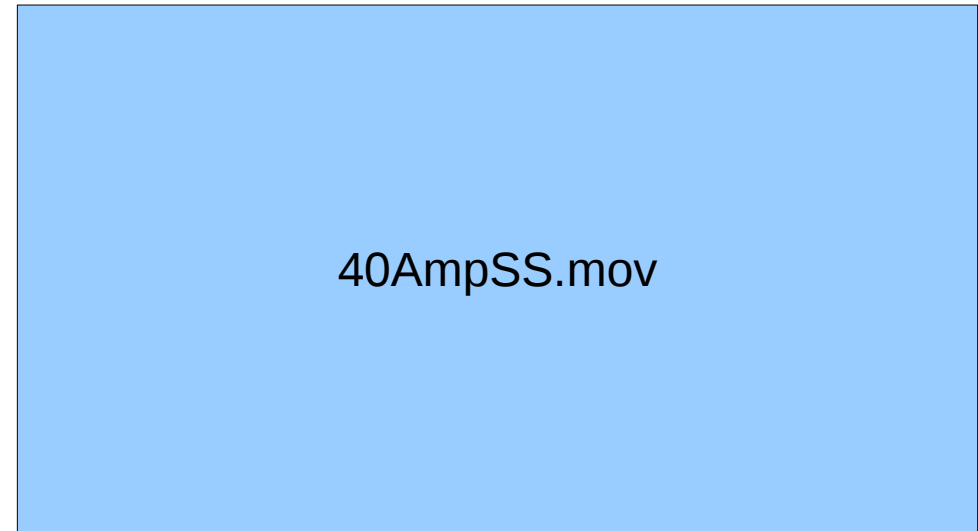


Results: Outline

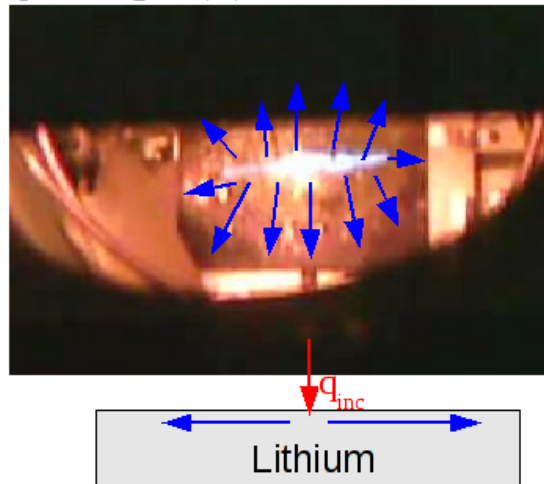
- Initial result – swirling flows observed
- Qualitative tests to establish flow origin
 - Direction and magnetic field
 - Material replacement
 - Spin down
- Quantitative assessment of data
 - Velocity measurements
 - Temperature for heat flux and interface reconstruction
- Comparison to theory

First Observation

- Flows in SLiDE were dominated by swirling flow
- At times, no surface swirling observed but sub-surface motion discernible
- Flows sometimes vigorous enough to “dry-out” and expose tray

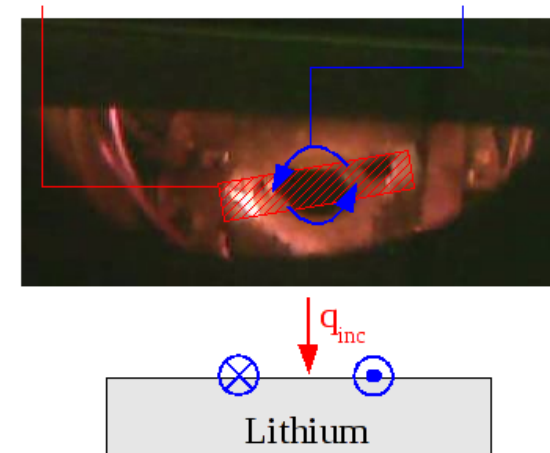


Expected grad(T) Based Force Vectors



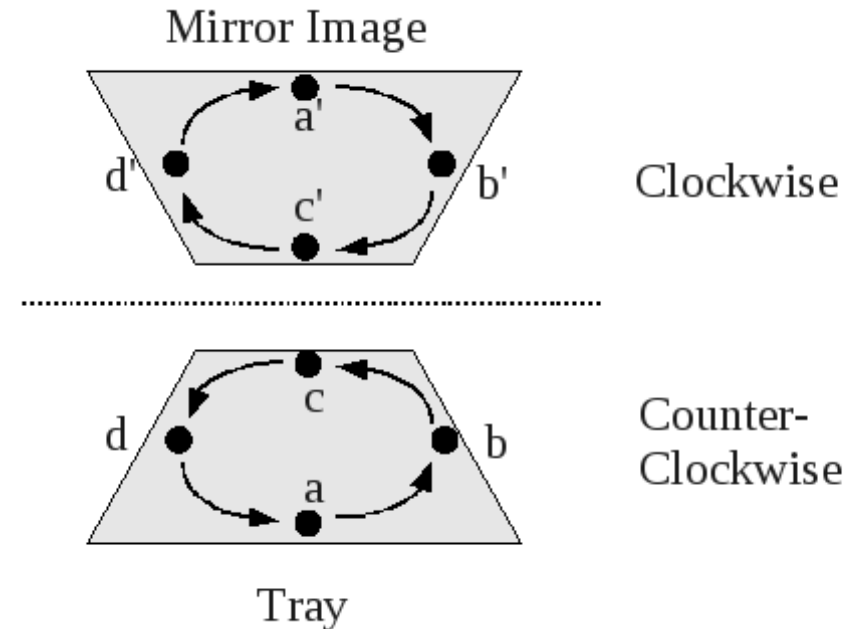
Beam Position

Observed Flow Direction



Qualitative Tests 1-3

- Magnetic field reversal
 - Flow direction reverses upon reversal of field
 - Flow is consistent and steady in swirl
- Flow direction consistent with TEMHD source
 - Mirror system reverses apparent sense of rotation
 - Magnets measured to determine direction
 - E-beam and TE have opposite rotation senses
- Addition of insulator halts any swirling flow
 - Quartz slides added between tray and lithium
 - No flow observed at all in these cases



Qualitative Test 4: Spin Down

- Based on time required for fluid to come to rest
 - Without magnetic field viscous damping stops flow
 - Magnetic fields in non-TE MHD destroy kinetic energy faster (slow quicker)
 - If thermoelectric currents exist, these will decay at a thermal time constant of the lithium-tray system
 - Maintained magnetic field will sustain flow
 - Turning magnetic field back on after viscous spin-down should induce motion once more
1. Obtain steady thermal conditions and flow
 2. Shut off beam and magnetic field
 3. Return to steady state with flow
 4. Shut off beam and maintain magnetic field
 5. Repeat test 1, but turn magnetic field back on after flow comes to rest

spinDown.mov



Spin Down Time Constant

- Spin down time requires thermal gradients to sustain currents
- Thermal time constant of the system can be estimated
 - Simple thermal resistance model applied
 - Measurements from the system used to make calculation
 - 78 seconds is thermal time constant
- Observed spin down time is equivalent to 2-3 thermal time constants

$$\Theta(t) = \text{Exp} \left[-\frac{t}{\tau} \right]$$

$$\tau = [(\rho C_p l)_{\text{Li}} + (\rho C_p l)_{\text{S.S.}}] AR$$

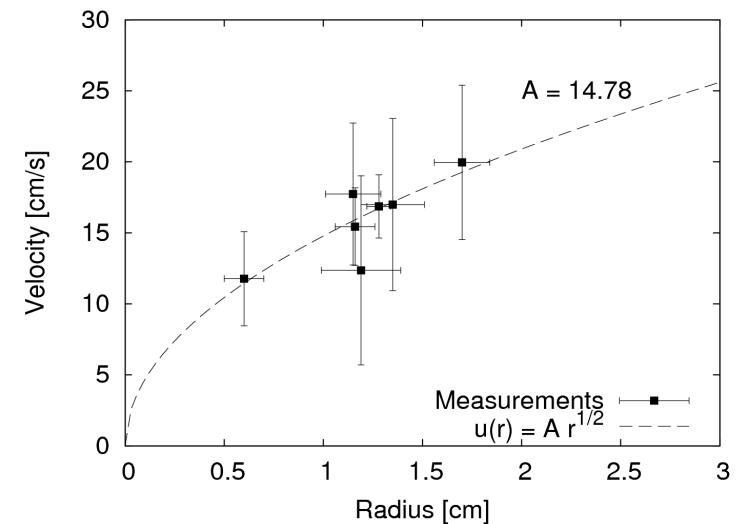
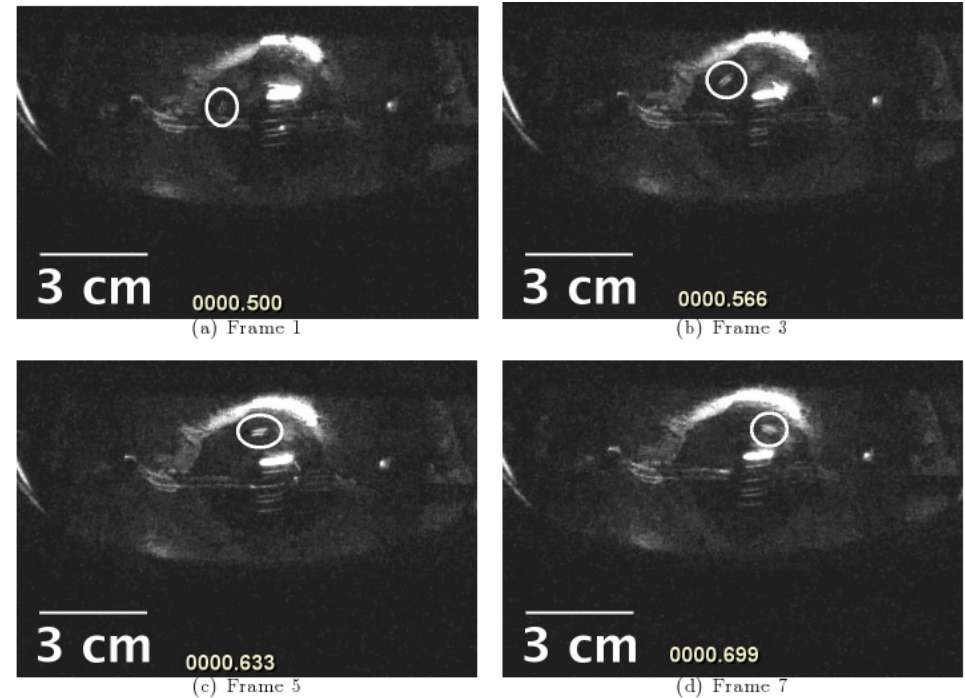
$$\tau = 78 \text{ seconds}$$

Case	Trial 1	Trial 2	Mean
Spin-down w/o magnetic field	3[s]	8[s]	6[s]
Spin-down w/ magnetic field	167[s]	210[s]	190[s]
Spin-up from spin-down?	yes	yes	—



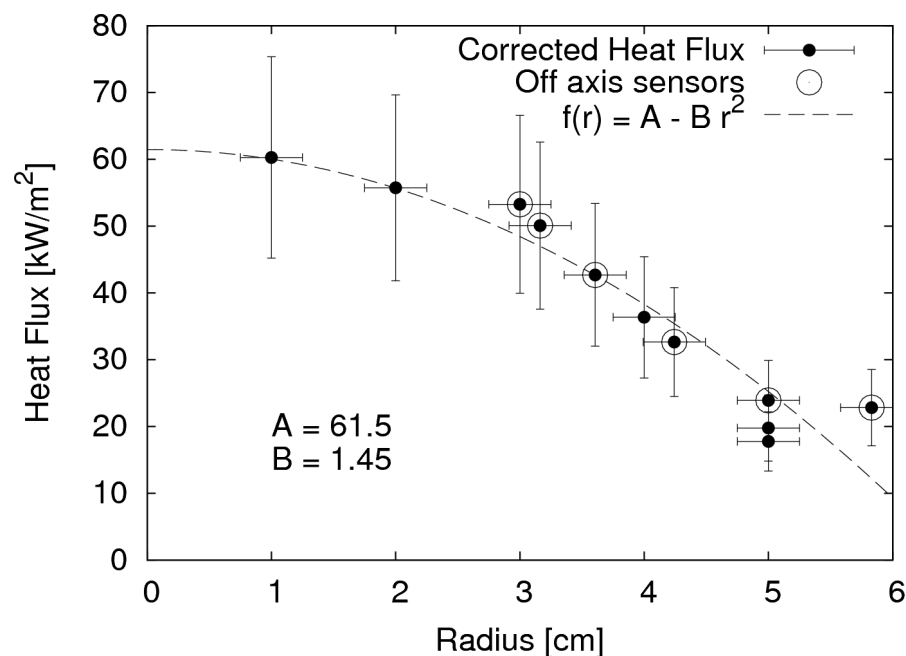
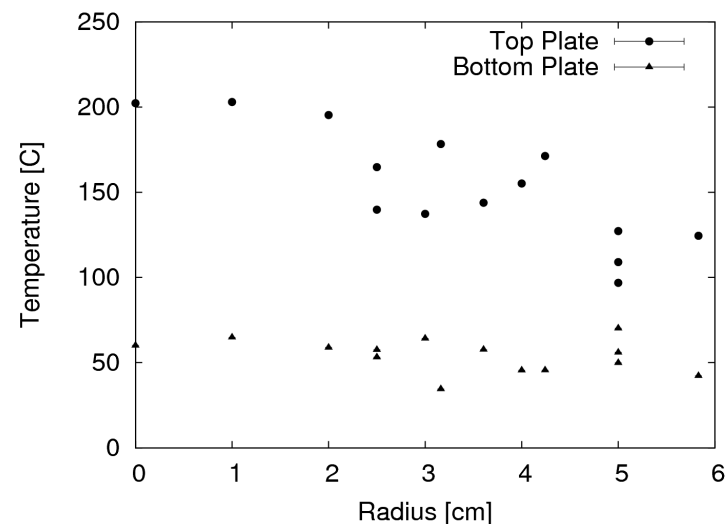
Quantitative Assessment

- Purpose: bring together thermal and velocity measurements
- Velocity measurements based on video analysis
 - Particles measured on a frame-by-frame basis
 - Multiple measurements made over course of particle visibility
 - Radial distance also measured
- Velocity and radius used to determine most likely velocity at $r = 1\text{cm}$
 - $u(r) \sim r^{0.5}$ based on Davidson swirling flow theory
 - Consistent with SLiDE data



Heat Flux Calculation

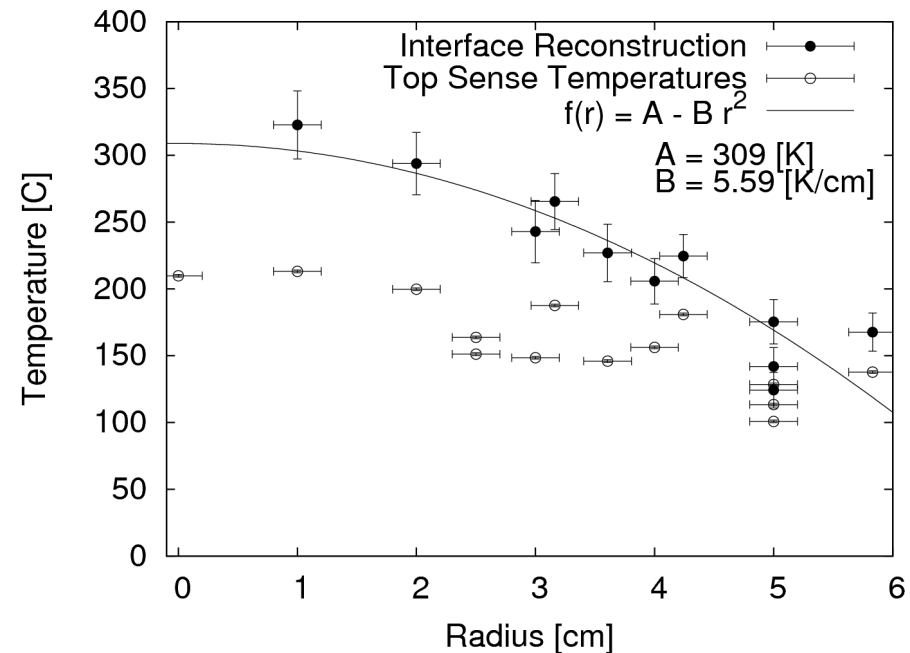
- Time series data reduced
 - Mean taken
 - Standard error calculated by standard formulas
- Fourier model applied to calculate heat flux
 - Scaling factor applied to account for tray warping
 - Radially symmetric pattern observed
 - Most obvious in “off-center” sensor sets
 - Radially symmetric pattern observed in all cases run
 - Some TC pairs eliminated due to tray damage directly underneath beam strike



Interface Reconstruction

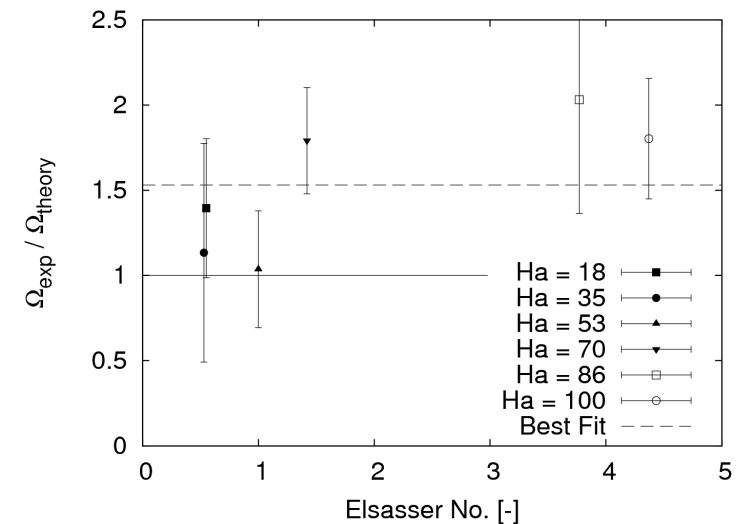
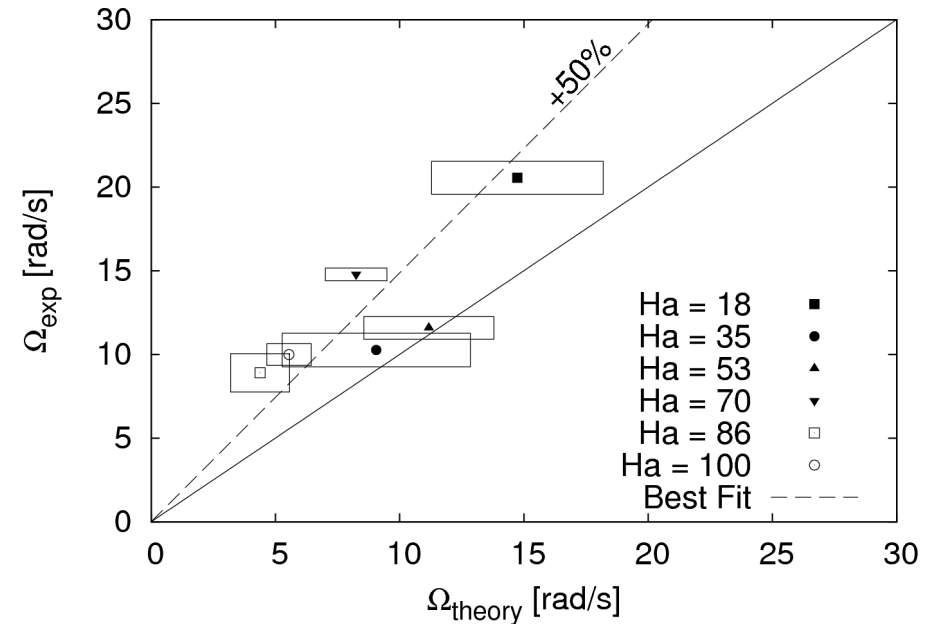
- Interface temperature reconstructed
 - Utilizes heat flux model and results of previous slide
 - Includes top plate temperature
 - Calibration data on effective distances
- Parabolic curve fit to data
 - Function form suggested by data
 - Results in easily calculable temperature gradient
 - Somewhat *ad hoc*
 - Parabolic form also needed for torque balance method (linear forces with radius)

$$T_{\text{int}} = T_{\text{top}} + \frac{1}{k}q \cdot Y_{\text{eff}}$$



Comparison to Theory

- Qualitative agreement (linear) between predicted value and theory
 - Data consistently *exceeds* predicted value
 - Factor of 3/2 is the linear least-squares best-fit of the data
- Lack of clear trends indicate systemic issue
 - Range of Hartmann (magnetic to viscous) and Elsasser (magnetic to Coriolis or rotational effects) numbers do not show clear trends
 - TEMHD common to all cases
- Most likely source of error is $\text{grad}(T)$ calculation
 - 1D Fourier Conduction *underpredicts*
 - Contact resistance between plates would increase the error associated with the 1D model



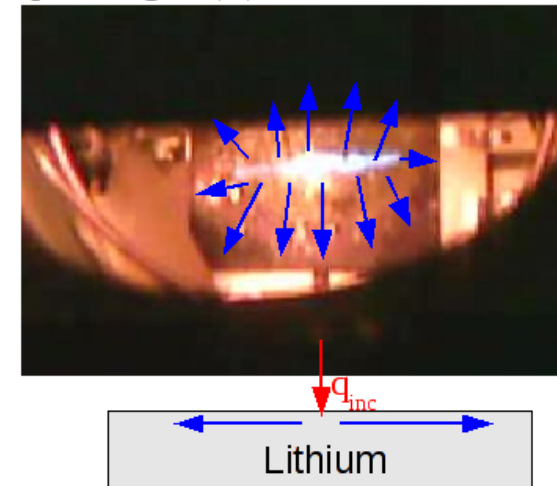
Discussion: Outline

- Quantitative comparison (immediately preceding)
- Interpretation of qualitative tests
- Evidence of swirling due to thermal measurements
- Evaluation of ratio between thermocapillary and thermoelectric MHD flows in SLiDE
- Generalization of TEMHD to TC driven flows and parameters of interest
- Implications and applications of TEMHD

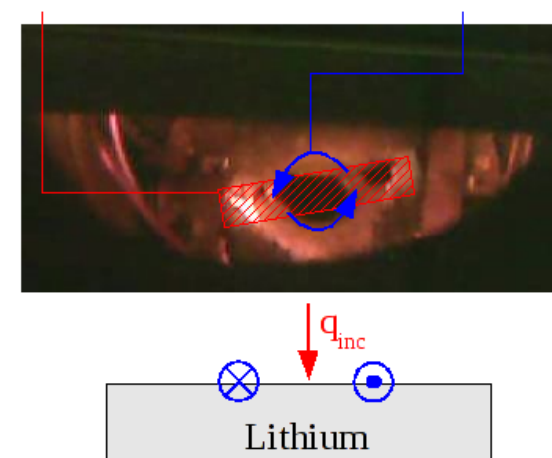
TEMHD Dominance

- TEMHD is consistent with all qualitative tests performed
 - Field dependence
 - Material replacement
 - Spin-down
- TC forces cannot sustain swirling flow as we observe it
- TC flow is observable in SLiDE in some parameters but not observed in most cases
- First *direct* observation of TEMHD flow

Expected grad(T) Based Force Vectors

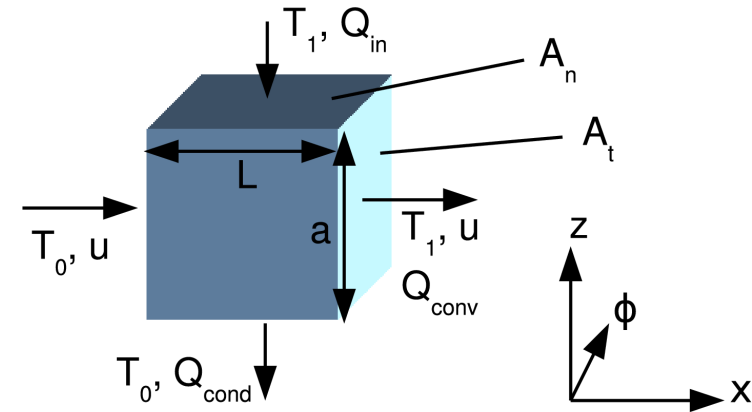


Beam Position Observed Flow Direction

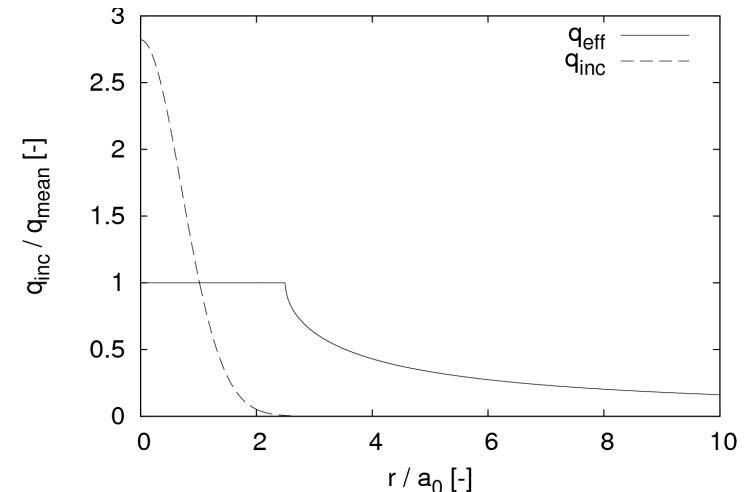


Cause of Radially Symmetric Temperatures

- Conduction and convection are both present
- Peclet number for swirling flow is large
 - 10 cm/s with 5mm depth, $Pe=24$
 - Even larger for deeper fills
- Results in “smeared out” heat flux on surface
- Meridional flow (r-z plane) has small Pe
 - Lower radial flow magnitude
 - Thin boundary layer
 - $Pe < 0.1$ for typical cases
- Convection dominated flow results in radial symmetry

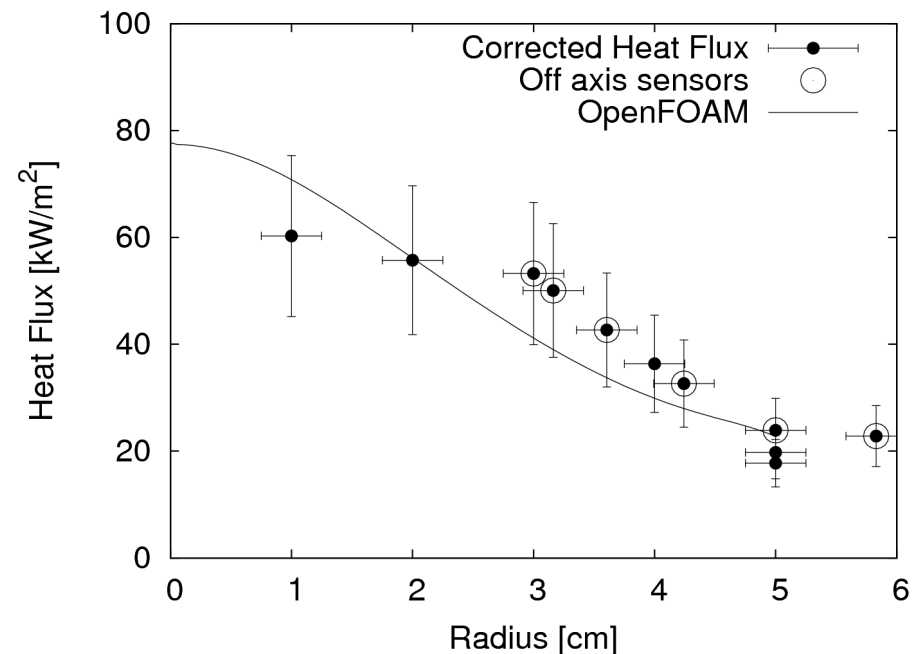
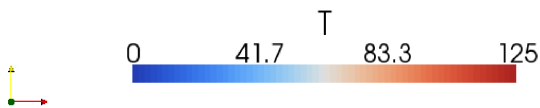
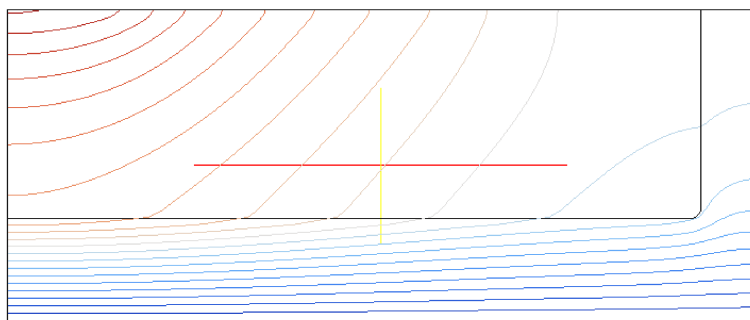
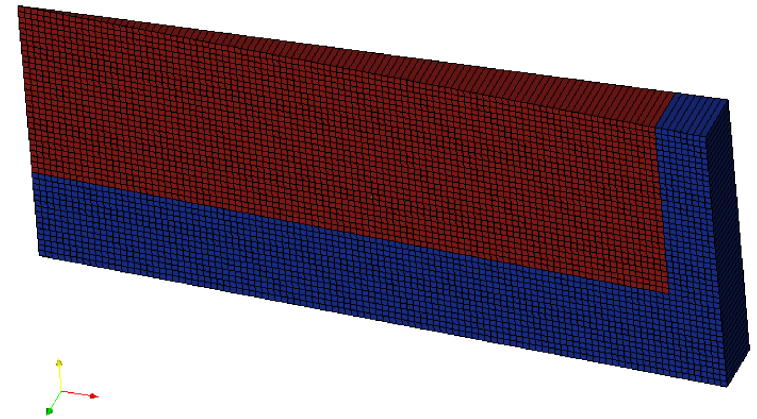


$$\begin{aligned}
 \frac{q_{in}}{k_{eff} \Delta T / a} &= 1 + \frac{f \rho_l c_{p,l} a^2 u}{k_{eff} L} \\
 &= 1 + \frac{au}{\alpha_{eff}} \cdot \frac{a}{L} \quad \mathfrak{Pe} = \frac{au}{\alpha} \\
 &= 1 + \mathfrak{Pe} \frac{a}{L}
 \end{aligned}$$



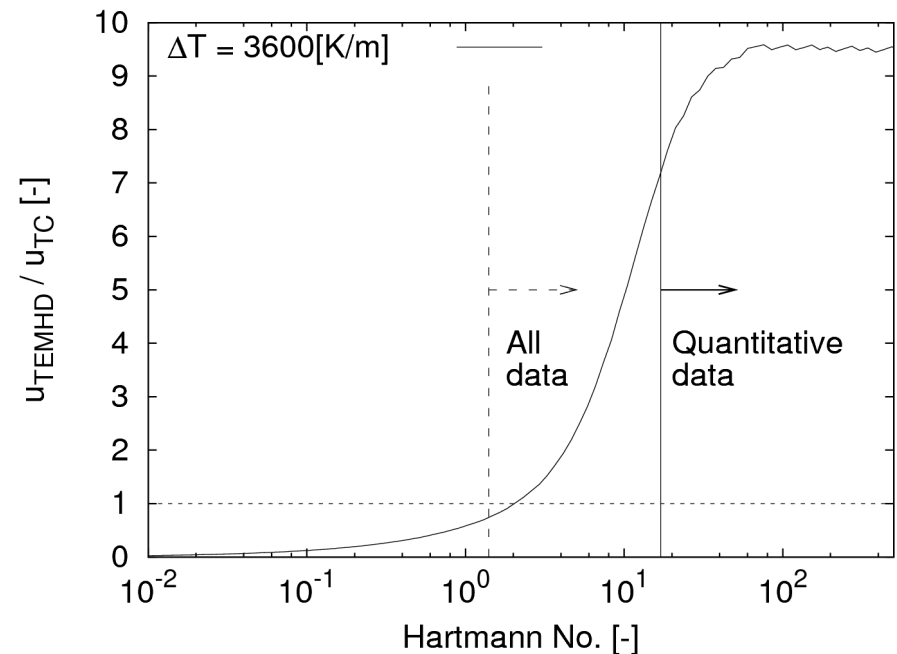
Computational Model

- OpenFOAM model created to verify effective thermal transport
 - Input heat flux is effective heat flux due to swirl
 - Back surface modeled as constant temperature (similar to copper block)
- Qualitative agreement between axisymmetric conduction model and data (quantitative to within error estimate)



Ratio of TEMHD to TC in SLiDE

- All data cases show evidence of swirling flow
 - TEMHD indirectly shown for $Ha > 1.4$ by temperature
 - TEMHD directly shown for $Ha > 17$
 - TC capable of being seen
- Ratio of TEMHD to TC velocity
 - Ratio = 1 indicates equal effectiveness
 - Ratio > 1 indicates TEMHD dominance
- All data consistent with this formulation



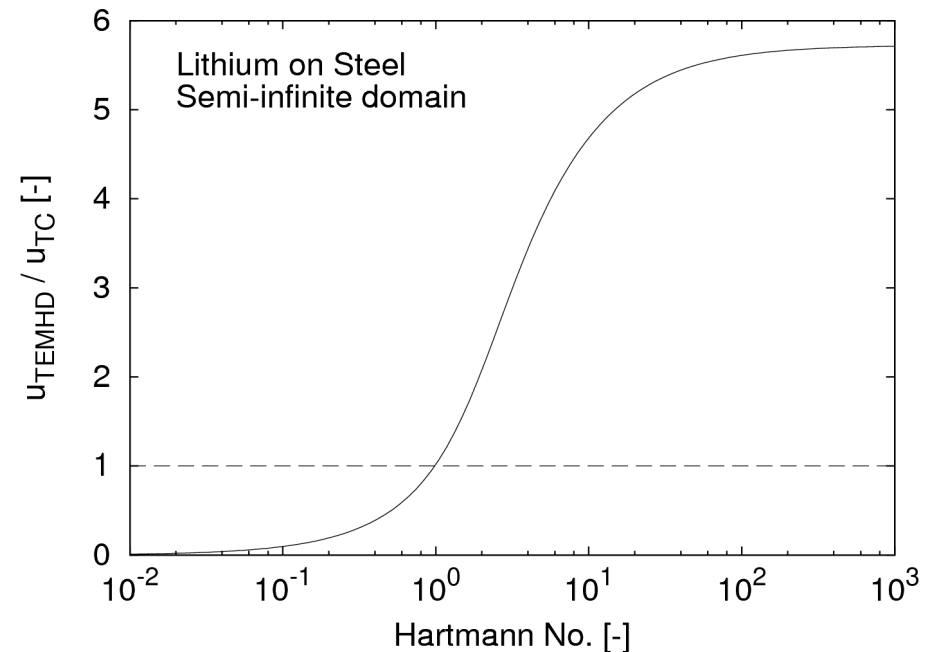
Ratio of Semi-Infinite Solutions

- Physics elucidated by analytical solutions to flow
 - “Open” geometry of semi-infinite solutions compared
 - Ratio depends on material parameters capture by dimensionless number, ζ
 - Also depends on container geometry captured in $F(Ha)$ function
- In Lithium-iron system, TEMHD dominance expected for $Ha > 1$

$$\frac{u_{TEMHD}}{u_{TC}} = \frac{P(\sigma\rho\nu)^{1/2}}{\gamma} F(\xi)$$

$$\text{where } F(\xi) = \frac{\xi - \tanh(\xi)}{\xi \tanh(\xi) + C \tanh^2(\xi)}$$

$$\zeta = \frac{P(\sigma\rho\nu)^{1/2}}{\gamma}$$



Comparison with Other Materials

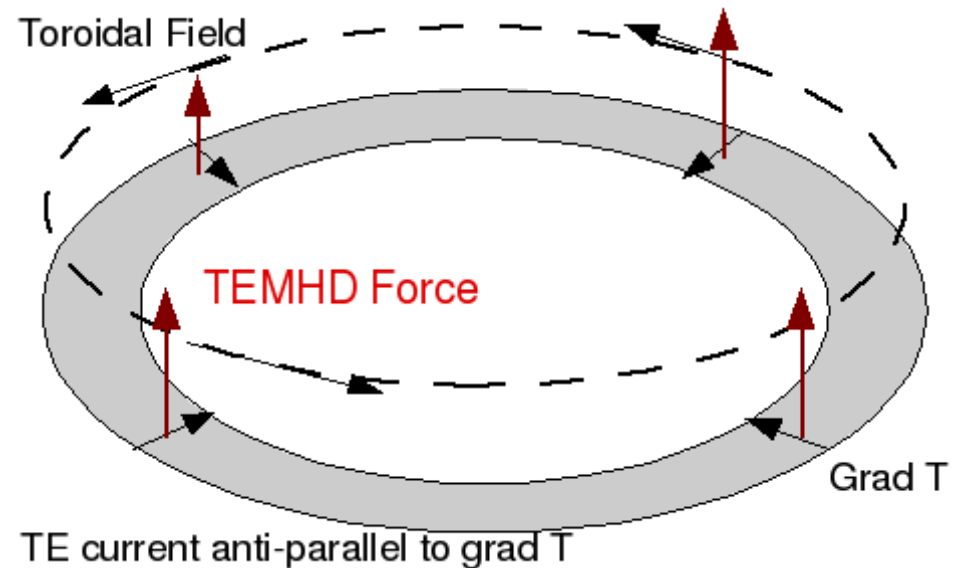
- Other materials can be compared based on available literature
 - Scant data for thermoelectric power of liquid metals
 - No data on fusion eutectics such as Pb-Li or Sn-Li
 - Exact relation between TEMHD and TC depends on container geometry (F function)
- Mercury systems would be dominated by thermocapillary forces
- Sodium systems could exploit TEMHD to great effect in large systems and modest magnetic fields

Metal Pair	$\sigma [1/\Omega \cdot \text{m}]$	$\rho\nu [\text{Pa} \cdot \text{s}]$	$\gamma [\text{N/m} \cdot \text{K}]$	$P [\mu\text{V}/\text{K}]$	$\zeta [-]$
Lithium-Iron	3.52×10^6	0.503×10^{-3}	0.147×10^{-3}	≈ 20	≈ 6
Lithium-Tungsten	3.52×10^6	0.503×10^{-3}	0.147×10^{-3}	≈ 10	≈ 3
Mercury-Copper	1.02×10^6	1.56×10^{-3}	0.302×10^{-3}	≈ 7	≈ 0.9
Mercury-Iron	1.02×10^6	1.56×10^{-3}	0.302×10^{-3}	≈ 15	≈ 2
Sodium-Iron	14×10^6	0.451×10^{-3}	0.09×10^{-3}	≈ 20	≈ 18
Sodium-Tungsten	14×10^6	0.451×10^{-3}	0.09×10^{-3}	≈ 15	≈ 13



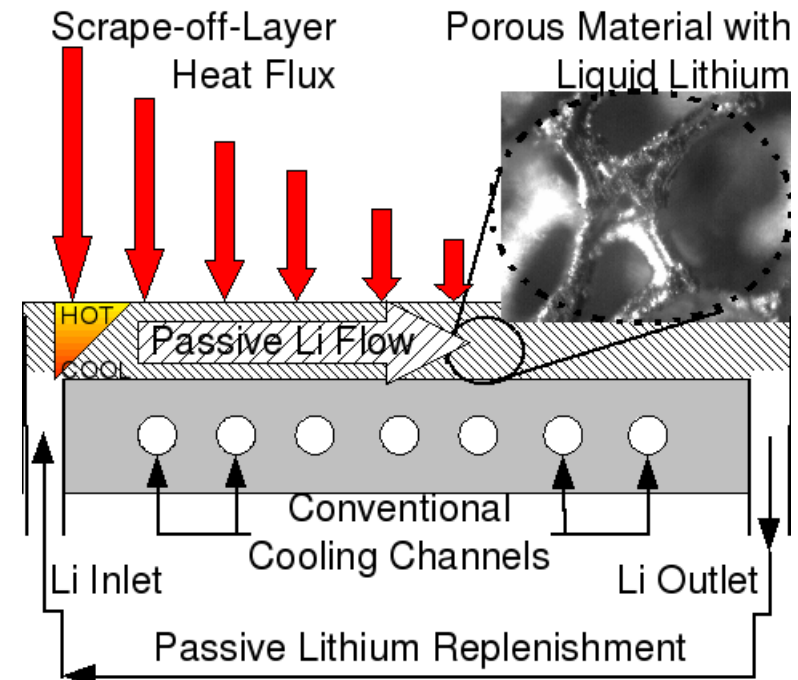
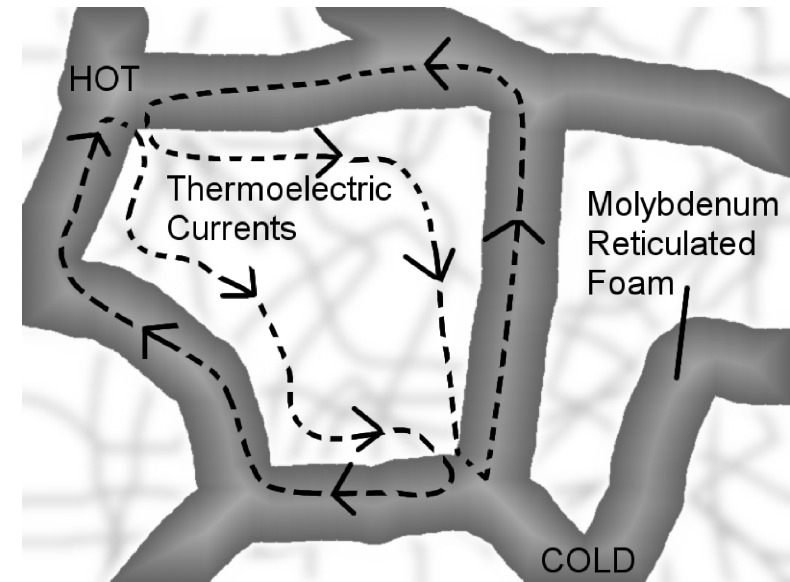
Implications and Applications 1

- Fusion systems will be subject to both forces
 - NSTX $B=0.5[T]$, inclination angle $\sim 5^\circ$ w.r.t. Horizontal
 - 1mm film has $Ha = 3.5$ – still TEMHD dominated but close to transition for Li-Fe system
 - Implications of multiple, thin metal layers not clear in TEMHD context
- Significant vertical forces developed due to horizontal magnetic field
 - Lithium subject to significant vertical body force
 - Dry out and ejection are possible outcomes depending on field direction



Application 2: Pumped Porous Material

- Utilize porous material infused with liquid metal
 - Porous material structure creates TE loops with liquid metal
 - Small pores create strong capillary forces at free-surface (similar to CPS)
 - Pore size can be engineered to optimize TEMHD effect
- Primary temperature gradient is due to incident heat flux
 - Secondary gradient due to heat flux shape
 - Pumps liquid metal radially
 - Passive replenishment system of liquid surface



Conclusions

- SLiDE designed, constructed and operated to examine free-surface liquid metal flows
- TEMHD determined to be dominant in SLiDE
 - First *direct* observation of TEMHD induced flow
 - Qualitative agreement between swirling flow theory and experiment
 - Quantitative prediction off by 50%, likely due to errors in interface reconstruction
- Theory of balance between TEMHD and TC induced flow developed
 - SLiDE observations consistent with theory
 - New dimensionless group identified describing this balance
 - Implications of TEMHD on fusion systems described
 - New applications for TEMHD described

Thank you for your time

Questions?

Backup Material

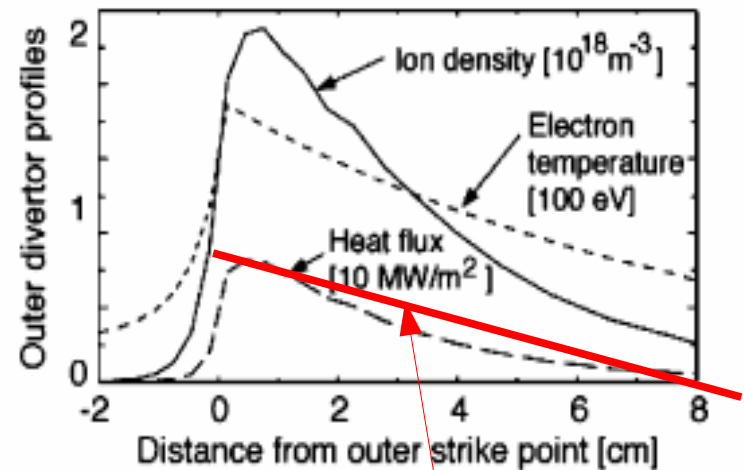
Backup slides

Liquid Lithium History

- Lithium proposed as pumping material for fusion reactors (Fraas, 1968 and McCracken, 1969)
- Tokamak Fusion Test Reactor (TFTR) obtains “supershots” with the use of lithium pellet injection (Strachan, 1987 and Snipes, 1992)
- Gettering and pumping of impurities and hydrogen studied in laboratory scale experiments (Sugai, 1995 and Baldwin, 2002)
- “Capillary Pore System” (CPS) developed in Russia on T11-M tokamak (Evtikhin, 2002) – successful limiter tests
- Helium retention experiments reported by UIUC (Nieto, 2003)
- **Li-DIMES experiments in DIII-D tokamak (Whyte, 2004) – plasma disruption due to lithium ejection**
- CDX-U experiments with liquid lithium limiters (2002-2007) – MHD activity decrease and improved confinement
- FTU (Italy, tokamak) and TJ-II (Spain, stellarator) use CPS and evaporation of liquid lithium respectively and see performance improvements
- NSTX experiments with lithium (2004-present) – ELM reduction and improved confinement

A Typical Fusion Heat Flux

- Magnetic configuration concentrates power in “diverted” plasma
 - Peak heat flux, steady-state typically 5-20 MW/m²
 - Radiant heat flux at solar surface is ~63 MW/m²
 - Transients can push the peak higher
- Thermally driven phenomena depend on heat flux gradients, not just peak values



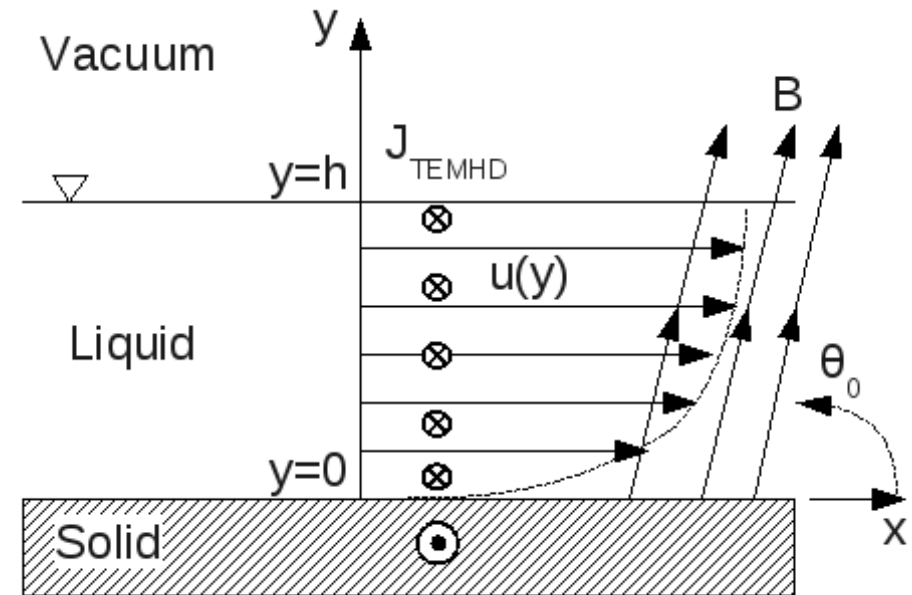
J.N. Brooks, et al. *J. Nucl. Mat.* 337-339 (2005) 1053-1057.

$$b = \frac{\partial T}{\partial x} \approx \frac{\partial q}{\partial x} \frac{L}{k}$$

Machine	Source	$\frac{dq}{dx} \frac{\text{MW}}{\text{m}^2\text{-m}}$	$b \frac{\text{K}}{\text{m}}$
DIII-D	Experimental (Disruption)	1250 [42]	$1.4 \times 10^{5*}$
ITER	Computational	—	$1.3\text{--}3.3 \times 10^4$ [43]
JET	Experimental	186 [44]	$3\text{--}9 \times 10^3$ [45]
JET	Experimental (Type I ELMs)	1300 [44]	$5\text{--}20 \times 10^3$ [45]
NSTX	Computational	100–800 [41]	$1\text{--}8 \times 10^{4*}$
NSTX	Experimental	100 [46]	$1 \times 10^{4*}$
TEXT-Upgrade	Experimental	—	5.8×10^5 [47]

TEMHD Formulation

- Same basic equations of motion
 - Navier-Stokes again used in semi-infinite domain
 - Alteration is inclusion of thermoelectric effect in Ohm's law
- Flow is perpendicular to temperature gradient
 - $\mathbf{J} \times \mathbf{B}$ results in Lorentz drive force
 - Resulting current flows through bulk of lithium and tray



$$\nabla \cdot \mathbf{V} = 0$$

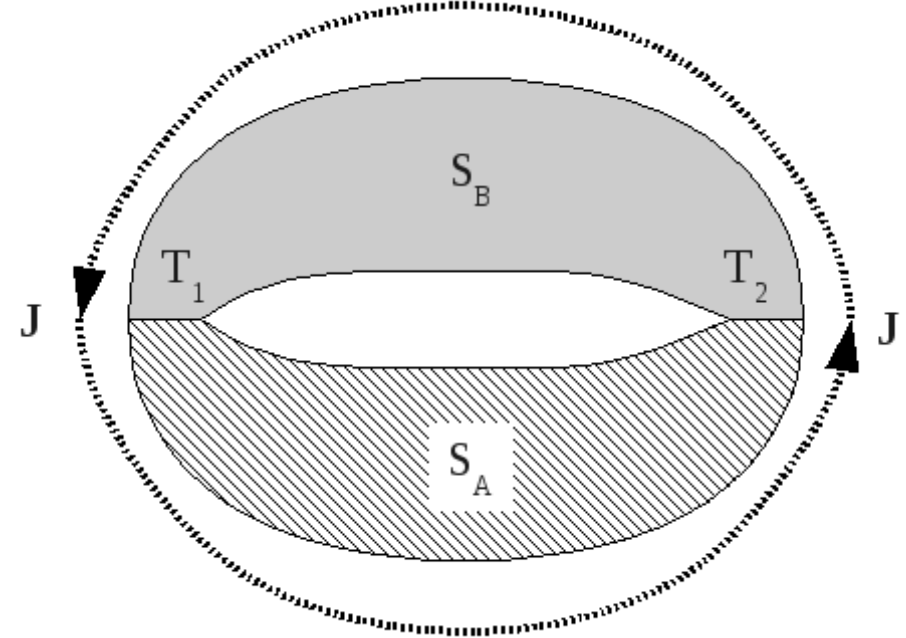
$$\rho \frac{D\mathbf{V}}{Dt} = -\nabla P + \mu \nabla^2 \mathbf{V} + \rho \mathbf{g} + \mathbf{J} \times \mathbf{B}$$

$$\rho C_p \frac{DT}{Dt} = k \nabla^2 T + \Pi + \frac{\mathbf{J} \cdot \mathbf{J}}{\sigma}$$

$$\mathbf{J} = \sigma (\mathbf{E} + \mathbf{u} \times \mathbf{B} - S \nabla T)$$

TEMHD Boundary Conditions

- Thermoelectric current depends on two items
 - Dissimilar materials
 - Temperature gradient
- Boundary condition at liquid-solid interface
 - Current density in fluid reduced by MHD current ($\mathbf{u} \times \mathbf{B}$)
 - Depends on surface tangential temperature gradient
- Thermoelectric power depends on both, wall and liquid



$$\mathcal{E} = \oint \frac{\mathbf{J} \cdot d\mathbf{l}}{\sigma}$$

$$\mathcal{E} = \int_{T_1}^{T_2} (S_B - S_A) dT$$

$$\mathcal{E} = \int_{T_1}^{T_2} P dT$$

$$\frac{j_{sw}}{\sigma_w} - \frac{j_s}{\sigma} + u_t B_n = P \frac{\partial T}{\partial s} = \frac{\partial \mathcal{E}}{\partial s}$$

Bödewadt-Hartmann Flow

- Bödewadt flow

- Rotating fluid over stationary disk
- Variation of Karman flow (rotating disk)
- Use Karman similarity variables to analyze

$$\frac{1}{r} \frac{\partial r u_r}{\partial r} + \frac{\partial u_z}{\partial z} = 0$$

$$u_r \frac{\partial u_r}{\partial r} + u_z \frac{\partial u_r}{\partial z} - \frac{u_\phi^2}{r} = -\frac{1}{\rho} \frac{\partial p}{\partial r} + \nu \left(\frac{\partial^2 u_r}{\partial r^2} + \frac{1}{r} \frac{\partial u_r}{\partial r} + \frac{d^2 u_r}{dz^2} - \frac{u_r}{r^2} \right) + \dots$$

$$\dots \frac{(\mathbf{J} \times \mathbf{B})_r}{\rho}$$

$$u_r \frac{\partial u_\phi}{\partial r} + u_z \frac{\partial u_\phi}{\partial z} + \frac{1}{r} u_r u_\phi = \nu \left(\frac{\partial^2 u_\phi}{\partial r^2} + \frac{1}{r} \frac{\partial u_\phi}{\partial r} + \frac{\partial^2 u_\phi}{\partial z^2} - \frac{u_\phi}{r^2} \right) + \frac{(\mathbf{J} \times \mathbf{B})_\phi}{\rho}$$

$$u_r \frac{\partial u_z}{\partial r} + u_z \frac{\partial u_z}{\partial z} = -\frac{1}{\rho} \frac{\partial p}{\partial z} + \nu \left(\frac{\partial^2 u_z}{\partial r^2} + \frac{1}{r} \frac{\partial u_z}{\partial r} + \frac{\partial^2 u_z}{\partial z^2} \right) + \frac{(\mathbf{J} \times \mathbf{B})_z}{\rho}$$

- Bödewadt-Hartmann flow

- Rotating flow with a magnetic field
- Non-dimensionalized system of equations results

$$u_r = \Omega r F(z/l)$$

$$u_\phi = \Omega r G(z/l)$$

$$u_z = \Omega h H(z/l)$$

$$p = 1/2 \rho \Omega^2 (r^2 + l^2 P(z/l))$$

- Elsässer No. - Balance of MHD to Coriolis force

$$F^2 + F'H - G^2 + 1 = \frac{\nu}{l^2 \Omega} F'' - 2\mathfrak{A} F$$

$$2FG + G'H = \frac{\nu}{l^2 \Omega} G'' - 2\mathfrak{A} G$$

$$HH' = \frac{1}{2l^2} P' + \frac{\nu}{h^2 \Omega} H''$$

$$2F = -H'$$

$$\mathfrak{A} = \frac{\sigma B^2}{2\Omega \rho}$$



Approximate Solutions for Velocity Profile

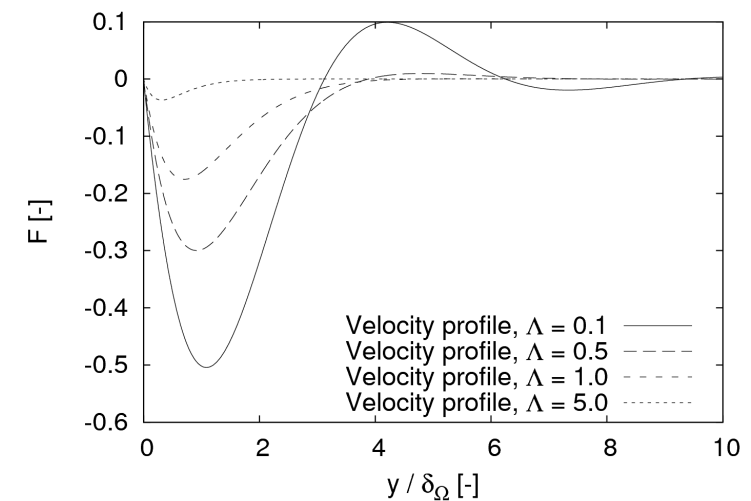
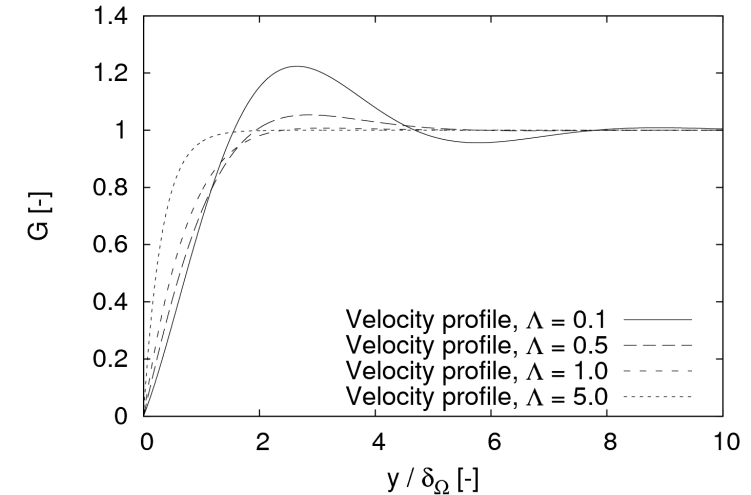
- Bödewadt-Hartmann flow analyzed – swirling flow above stationary plate in a magnetic field
- Make use of Davidson, 2002 approximate solutions
 - Linearized equations about core flow solution
 - Compares well with direct numerical integration
 - Aids further analysis

$$G = 1 - \text{Exp} \left[- \left(\hat{R} - \frac{H_\infty}{2} \right) \frac{z}{\delta_\Omega} \right] \cos \left(\frac{z}{\hat{R}\delta_\Omega} \right)$$

$$F = -\text{Exp} \left[- \left(\hat{R} - \frac{H_\infty}{2} \right) \frac{z}{\delta_\Omega} \right] \sin \left(\frac{z}{\hat{R}\delta_\Omega} \right)$$

$$\hat{R} = \left[\hat{\alpha} + (1 + \hat{\alpha}^2)^{1/2} \right]^{1/2}$$

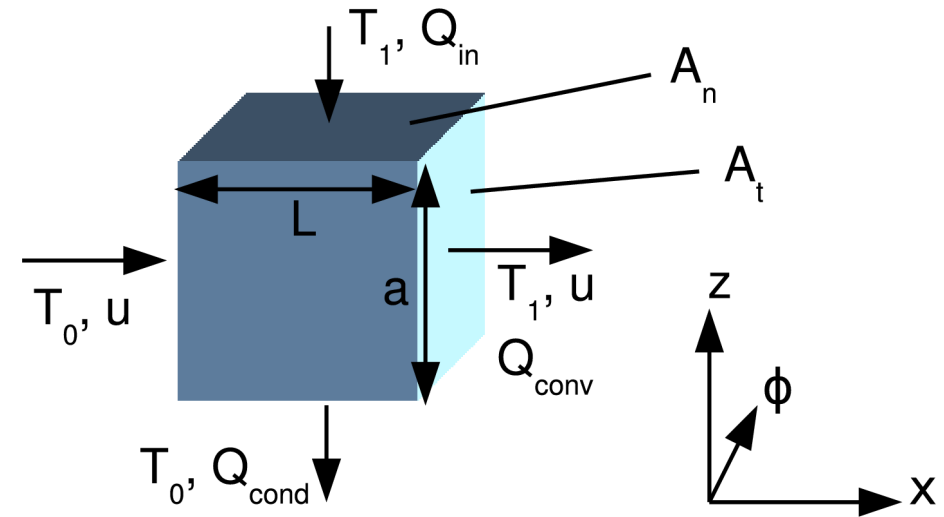
$$\delta_\Omega = l = \left(\frac{\nu}{\Omega} \right)^{1/2}$$



Distance from wall →

Thermal hydraulics of the Flow

- Liquid metals typically conduction dominated
 - High thermal conductivity compared to water and air
 - Significant velocity needed for effective energy transport
- Simple control volume illustrates
 - Peclet number is balance between convection and conduction
 - $Pe \gg 1$ means convection dominated thermal transport
- Fast flows will alter the temperature solution significantly



$$Q_{in} = Q_{cond,l} + Q_{cond,s} + Q_{conv}$$

$$= k_{eff} A_n \frac{\Delta T}{a} + \rho_l C_{p,l} A_t \Delta T u$$

$$\frac{q_{in}}{k_{eff} \Delta T / a} = 1 + \frac{f \rho_l c_{p,l} a^2 u}{k_{eff} L}$$

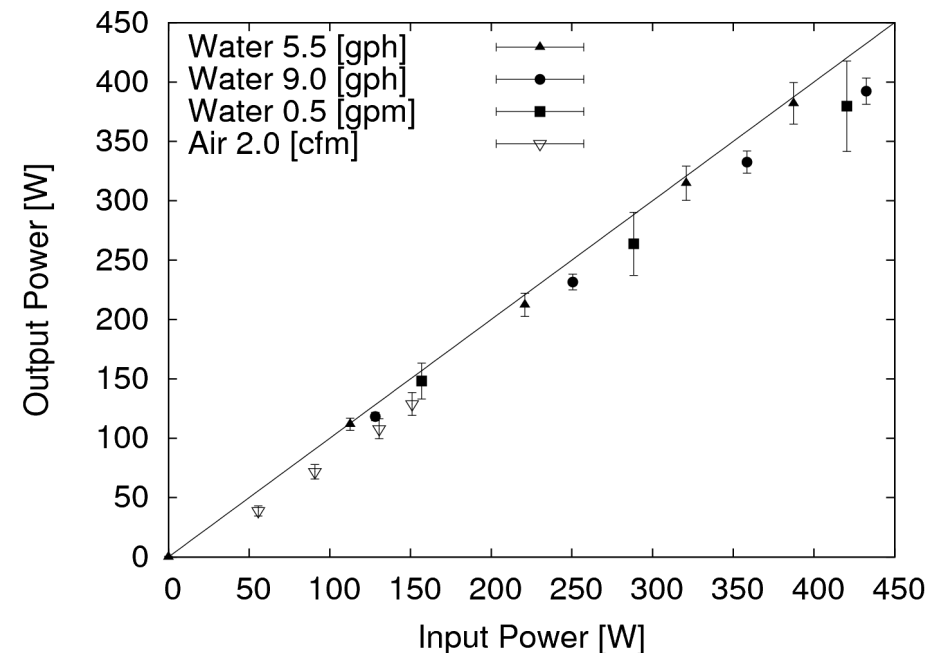
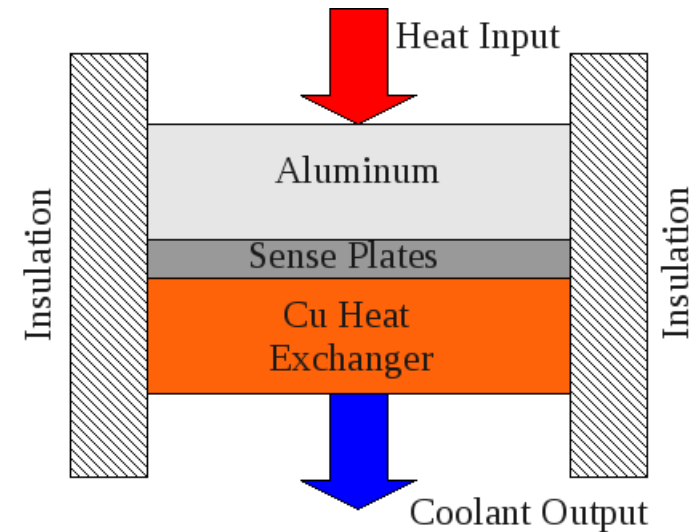
$$= 1 + \frac{au}{\alpha_{eff}} \cdot \frac{a}{L}$$

$$= 1 + \mathfrak{Pe} \frac{a}{L}$$

$$\mathfrak{Pe} = \frac{au}{\alpha}$$

Tray Calibration

- Calibration rig
 - Electrical heater attached to ~2cm aluminum block
 - Well insulated
 - Aluminum and copper block temperatures monitored as well as input power to heater
- Calorimetry calculations performed
 - Based on enthalpy change
 - Moist air calculations necessary because of building supply
- Data sets form basis for Fourier heat transfer model



Applications 3 and 4

- TEMHD pumping without insulating breaks
 - MHD pumps typically utilize insulating sections to force current through the liquid metal
 - TEMHD could be used in a duct without changing materials
 - Elimination of ceramic materials lessens potential for failure
 - Reduced possibility for contamination
- TEMHD induced swirl in metallurgical systems
 - Swirl already demonstrated with SLiDE
 - Rotating magnetic fields (RMF) currently utilized to induce swirl in crucibles
 - RMF is reduced by skin losses in crucible walls
 - TEMHD could be utilized if the liquid metal melt could withstand the impurity and avoid skin losses with a static field